WHY BOTHERING TO MEASURE STELLAR ROTATION WITH COROT ?

M.J. Goupil[1], A. Moya[1], J.C. Suarez[1], J. Lochard[1], C. Barban [1], J. Dias do Nascimento[3], M.A. Dupret[1], R. Samadi[1], A. Baglin[1], J.P. Zahn[4], A.M. Hubert[5], S. Brun[6], L. Boisnard[7], P. Morel[8], R. Garrido[9], S. Mathis[4], E. Michel[1], J. Renan de Medeiros[3], A. Palacios[10], F. Lignières[2], and M. Rieutord[2]

[1] *LESIA, UMR CNRS 8109, Observatoire de Paris, France*
[2] *Observatoire de Midi-Pyrénées, Toulouse, France*
[3] *DFTE- Natal Departamento de Fsica Terica e Experimental, Brazil*
[4] *LUTH, Observatoire de Paris, France*
[5] *GEPI, UMR CNRS 8111, Observatoire de Paris, France*
[6] *CEA, Saclay, France*
[7] *CNES, Toulouse, France*
[8] *Observatoire de la Côte d'Azur, Nice , France*
[9] *Instituto de Astrophysica de Andalousia, Spain*
[10] *GRAAL, Universite de Montpellier, France*

ABSTRACT

One important goal of the CoRoT experiment is to obtain information about the internal rotation of stars, in particular the ratio of central to surface rotation rates. This will provide constraints on the modelling of transport mechanisms of angular momentum acting in radiative (rotationally induced turbulent) and convective zones (plumes, extension beyond convectively instable regions). Relations between the surface rotation period and age, magnetic activity, mass loss and other stellar characteristics can also be studied with a statistically significant set of data as will be provided by Corot. We present various theoretical efforts performed over the past years in order to develope the theoretical tools which will enable us to study rotation with Corot.

1. INTRODUCTION

All stars rotate more or less rapidely and many are actually rotating quite fast. Many issues concerning rotating stars are not fully understood yet and under investigation : what is the structure of a rotating star? what is its rotation profile? what are the transport mechanisms of angular momentum and of chemical elements ? As some mixing is driven by rotation, to what extent does it depend upon the rotational history of the star? Which physical processes control the behavior of rotation along the HR diagram? What is the effect of rotation on mass loss? What are the consequences of rotationally induced mixing on the yields and then on the formation of successive star generations? How does magnetic braking affect rotation ? Does rotation control dynamo process and stellar activity? More generally what are the consequences of the interactions between rotation, magnetic field and atomic diffusion processes on the structure and the evolution of stars? Hence, rotation can seldomly be studied alone as it is connected with many other processes such as mixing, activity and compete with many other processes: turbulence, gravitational settling and/or radiative diffusion. As for the Sun, seismology is expected to provide some constrains on these various physical processes at play in stars and obtain clues about how to model them. Seismology is expected to provide information on the rotation itself and on the structure of the star. However, rotation is able to modify the oscillation frequencies and changes differ from one type of star to another, depending on the magnitude of the rotation rate and the type of excited oscillation modes. Determining effects of rotation on stellar oscillations can then be seen as a field of research on its own.

Many observational and theoretical efforts have been carried out over the past decade to provide answers to some of the above questions. The aim of the present paper is to give an overview of various theoretical developments which have been carried out in recent years *in preparation of the scientific return from CoRot experiment.* Stellar rotation and activity are two quantities which are accessible to Corot accurate measurement capabilities for many stars of various classes (ie wide mass and age ranges). The interested Corot community has therefore gathered in a team, AcRoCoRot, in order to coordinate their efforts about these two general issues. Two meetings have taken place during the Corot Brazil workshops in 2004 and 2005 as Bresilian are deeply involved in AcRoCoRot projects. Presentations

given during these meetings can be found on line at the site http://ace.dfte.ufrn.br/corot/index.html Several presentations during both meetings concerned rotation as will be mentionned later on in this review.

The paper is divided into 4 parts: Part I presents some *additional programs* related to stellar rotation which have been proposed. These projects basically require the determination of the surface rotation period for as large a number of stars as possible. As for the *core program*, proposals related to rotation will need the knowledge of internal rotation gradients for instance and will require the accurate measurements of as large a number of frequencies as possible for a few stars.

Part II briefly explains the tools which have been developped in order to compute oscillation frequencies of rotating stars. Indeed, differences between computed and observed frequencies in fine must come from differences between the stellar model and the real structure of the star and not from inaccuracy in determining the theoretical oscillation frequencies. Different levels of approximation are available and discussed depending on the magnitude of the rotation, whether it is fast or not. One important issue then is to determine how fast is fast in the present framework.

In Part III, we consider imtermediate mass and massive stars, more precisely A-B type stars such as δ Scuti and β Cephei stars which are suitable for testing rotational mixing of type I . Effects of these processes upon oscillation frequencies must be quantified by means of comparison with frequencies of nonrotating models. As these stars do not lose angular momentum, they rotate fast and effects of rotation on frequencies are important. Perturbation techniques as well as nonpertubative approaches have been developped in order to be able to study the oscillations of these stars and will be presented. The domain of validity of perturbation techniques will also be discussed.

In part IV, we discuss the case of solar-like stars. As the Sun, these stars oscillate with high frequency p-modes which are stochastically excited by turbulent convection in outer layers. Their oscillation spectra are characterised by a large number of small amplitude frequencies, a number of equal spacings. These stars are usually known as slow rotators. However we will see that effects of rotation on some frequency spacings at the needed accuracy level are not negligible and must be taken into account for further correct seismic interpretations of the data.

Finally some conclusions are drawn in Sect.9

Determinations of rotational splittings and inclination angles are left to another paper in this volume. Some parts of the present paper are not exhaustive

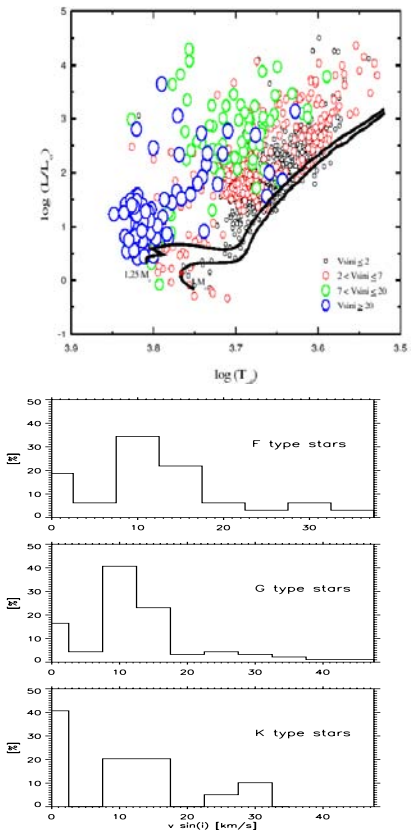

Figure 1. **top:** *Distribution of* $v \sin i$ *in the HR diagram obtained with Coravel measurements (De Medeiros, Mayor, 1999). Tracks are from do Nascimento et al. (1999) (taken from Do Nascimento and De Meideros, 2004, AcRotCoRoT) .* **bottom pannels:** $v \sin i$ *histograms for F-G-K stars (taken from Goupil et al. (2003), based on data from Cutispoto et al. (2002)).*

as they are treated in other contributions in this volume. Because of an expanding amount of work about stellar rotation, the present paper cannot be exhaustive and is therefore biased by the interests of the authors which do apologize for that.

Part I: What is at stake ?

1D standard models reproduce the gross features of evolution. However it is well known that hydrodynamical processes such as turbulent convection are not well modelled. In addition, observations require to go beyond standard models, particularly they show a need to include additional mixing. Two developement directions beyond standard evolution modelling are currently being followed:

- modelling transport processes and their consequences with prescriptions derived from physical

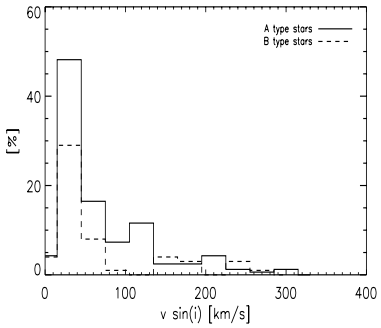

Figure 2. $v \sin i$ histograms fro A-B stars (taken from Goupil et al (2003), based on data from Royer et al. 2002a,b)

first principles, 3D numerical simulations, laboratory experiments or observations. The results of such modelling is implemented 1 D evolutionary models. Along this line, effects of rotation are taken into account in several evolutionary codes (Geneva code, Maeder et Meynet, 2004; STAREVOLV, Palacios et al. 2003; Cesam, Moya et al 2006).

- 2D numerical approach. A few 2D evolutionary models are currently being developed with inclusion of microphysics to become more realistic (Roxburgh 2004, ESTER code: Rieutord et al. 2005, Rieutord 2006)

Outcome of these modellings must be tested with observations. One information at our disposal can be the surface rotation rate. This enables to study relations between surface rotation (determined through microvariability) and other stellar parameters (Sect.2 below). More information about stellar rotation can in principle come from seismology. However rotation can significantly affect stellar pulsations. The centrifugal force distorts the shape of the star and modifies its equilibrium structure. Coriolis force directly affects the oscillatory motions. In order to take fully advantage of pulsations, one must first establish to what extent they are affected by rotation. A first approach assumes that rotation is slow enough that it can be treated as a perturbation both for the equilibrium structure and for the oscillations (Sect.3.3.1 below). The 2nd approach is valid for any rotation and consists in solving a 2D numerical system which include effects of rotation (Sect.3.3.2). The approach has been developed to apply to pressure modes (Espinosa et al, 2004; Lignières et al 2006; Reese et al 2006) as well as to gravito-inertiel modes (Dintrans, Rieutord, 2000).

2. ONE SINGLE INFORMATION : $P_{ROT,SURFACE}$ FOR MANY STARS

Fig.1 (presented by Do Nascimento, 2005 AcRot-CoRoT) displays the distribution des $v\sin i$ in the HR diagram obtained from Coravel instrument (De Meideros, 1999; Do Nascimento and de Meideros 2005). Some Corot additional programs propose to determine the surface rotation period for a large sample of stars (Do Nascimento, de Meideros et al.; Favata et al., AcroCorot 2005). This will enable to study the behavior of the surface rotation of solar-type stars from the main sequence to the giant branch. Statistical studies will be used to obtain relations between the surface rotation rate and other stellar quantities such as luminosity, mass, age, and chemical elements.

Determination of the surface rotation period will be obtained with CoRoT through periodic variability indicative of the presence of spots at the surface of the stars. Using a model with multispots at different latitudes, it could even be possible to study the latitudinal surface differential rotation (Petit et al., 2004, 2006; Donati et al. 2003; Marsden etal. 2006; Reiners et al 2003; Streissmeier et al. 2003) from the (micro)variability of the star as measured with CoRoT as explained by Cutispoto (2005, AcRot-CoRoT)

2.1. Age-activity -rotation relation for late type stars

The basic idea is that chromospheric activity is triggered and sustained by rotation in convective envelope of solar like stars. Because of rotation breaking by a magnetised stellar wind, rotational velocities decreases with age as well as activity for single stars.

Low mass stars at the very beginning of the main sequence show a high dispersion in rotational velocity and therefore in their chromospheric-activity level as a result of their different PMS history. However magnetic breaking forces very rapidely uniform rotational velocities. Issues then are for instance 'does a t^a law hold for late type stars and more massive stars as well? which value must be chosen for a ?'

Another important issue is to study the relation between rotation, activity and convection in stellar outer layers (Aigrain et al., Baudin et al., 2005, AcRoCoroT). This relation can be studied in a diagram activity level versus Rossby number where the Rossby number is the ratio of the rotation period (obtained with Corot) and the turn over time of the turbulent eddies (Fig.3). The activity level can be assessed with photometric variability which from ground is detected at the level of $10^{-2} - 10^{-3}$ (Fig.3). A level down to $10^{-3} - 10^{-4}$ is expected to be reached with Corot. This will allow to extend the

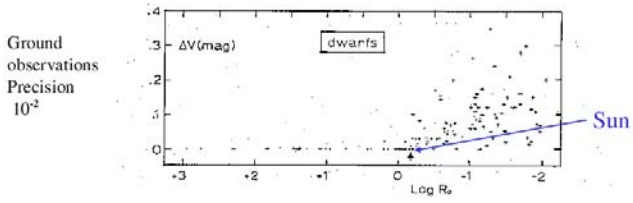

Figure 3. Observed activity-rotation relation for low mass stars. Both activity and Rossby number (rotation period) are measured through photometric variability.

study of the magnetic activity to stars earlier than G8.

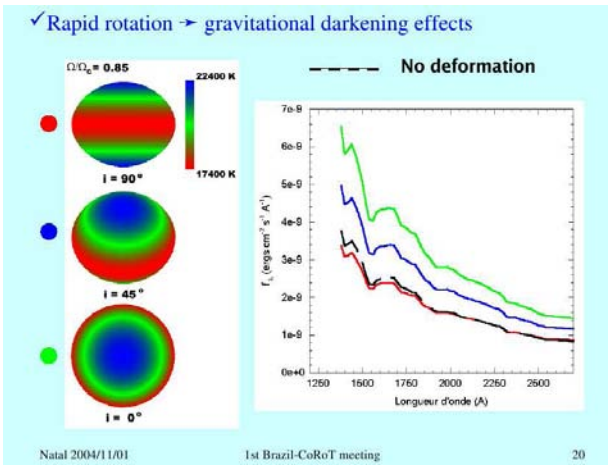

Figure 4. A schematic representation of darkening effect due to fast rotation. Polar regions are hotter than the equatorial ones. The line profiles seen from the poles and from the equator differ. This dependence upon the inclination angle must be taken into account when deriving stellar parameters from model atmospheres. (from Hubert el al., 2004, AcRo-CoRoT)

2.2. Mass loss-rotation relation for massive stars

For massive stars ($9 - 20 M_\odot$) (O-B stars), the evolution of surface rotation is affected by mass loss and/or internal transport mechanisms (Meynet & Maeder 2000; Meynet& Maeder, 2005). Of particular interest here are B_e stars as presented by Hubert et al. (2004) at the 1st Corot Brazil workshop. Be stars are main sequence or slightly evolved B stars surrounded by an equatorially concentrated envelope, fed by discrete mass loss events. Be stars usually rotate rapidly ($\Omega/\Omega_c \geq 0.80$) however their rotation rates do not reach the break-up velocity. The issue is therefore to identify the mechanism at the origin of the nonregular mass losses in these stars. As these stars are non radial pulsators, one question is whether pulsations do trigger direct mass loss events. Be stars also show stellar and circumstellar activity. Projected rotational velocities have been determined for hot and massive (O type) stars (Penny et al 2004; Gies, Huang 2004). One often encounters stars with $v/v_{crit} \sim 0.9$ (Townsend et al., 2004) which means that $v_{esc} \sim c_s$ the escape velocity is of the same order of magnitude than the sound speed, this indicates that a nonradial pulsation driven wind can indeed be efficient for these stars (Owocki et al., 2004). Magnetic field (several hundred of gauss) have been detected at the surface of these stars (Neiner et al 2003). Activity of magnetic origin has also been proposed as a mechanism that could give rise to the additional amount of angular momentum needed to eject material. Metallicity can also play a role in the sense that at low metallicity, mass loss is smaller, hence less loss of angular momentum and the stars rotate faster and could reach more easily the break up velocity than stars with same age and mass but with solar metallicity (Maeder, Meynet, 2001). Observations are carried out with the purpose to confirm these statements (Martayan et al. 2006).

In order to investigate the interrelation between fast rotation, magnetic field, pulsations, metallicity and mass loss in Be stars, accurate determination of stellar parameters (location in the HR diagram, v sin i, metallicity) is required. This is currently done for a number of Be stars in the set of Corot possible target stars (Fremat et al., 2006).

These stars are fast rotators and gravitational darkening effect are no longer negligible (Fig.4). This is confirmed by recent interferometric observations which starts to yield information about the oblate shape of rotating stars and gravitational darkening (Domiciano de Souza, 2005). As the poles are hotter than the equator, some lines will tend to form more easily at the poles rather than at the equator; hence the line profiles are not the same when seeing from regions near the pole or equatorial regions. They are inclination angle dependent and one has to take this effect into account in the models when deriving the stellar parameters of rapid rotating stars (Zorec et al 2005, Fremat et al 2005, Martayan 2005 phD). When studying the Be star ω Orionis, Neiners et al (2003) for instance used the code FASTROT (Fremat et al 2005) which has been developped for providing grids of theoretical spectra taking into account the effects of a rapid rotation and inclination angle on the line profiles.

Meynet and Maeder (2005) stress that stellar models with rotation predict that for stars with mass less than $< 12 M_\odot$, mass loss is small and internal mechanisms transports are dominant in controlling

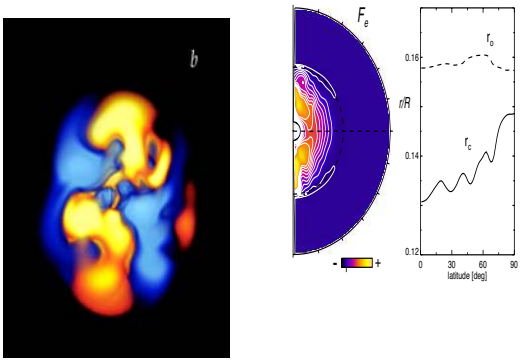

Figure 5. Numerical simulation of the inner 30% *in radius of A type 2* $M_\odot$ *star. The rotating convective core extends over approximately* 15% *of the radius .* **left:** *a 3-D rendering of the radial velocity is shown near the equatorial seen from above at a given time. Blue regions: descending flows; red ones: ascending flows. Overturning motions have time scales of order 1 month ie about the rotation period.* **right:** *enthalpy flux: a latitude dependence is clearly visible. The mixed central region when including effects of both penetration and overshoot keeps a nearly spherical shape in average. Extension of the mixed central region is in average* $\sim 0.2H_p$*. (taken from Browning et al 2004)*

the time evolution of the surface rotation velocity. They suggest to study of the behavior P_{rot} in function of the distance from the Zams which can provide constrains on the tranasport processes.

3. ONE STAR: MANY OSCILLATION PERIODS

As mentionned earlier, open questions are whether the rotation profile is shellular, what is the strength of the radial differential rotation and the extention of the central mixed regions when they are convective and rotating Hence with Corot, goals are – to identify *regions of uniform rotation* and regions of *differential rotation* (depth, latitude dependences) inside the star, – to determine $\Omega_{core}/\Omega_{surf}$ that-is whether the core is rotating faster than the surface and in this case by what amount. This type of information can in primciple best come from seismology, provided there are enough oscillation frequencies detected and accurately measured. These strong requirements met for a few stars in the Corot observing program.

3.1. Extension of rotating convective core

Intermediate mass stars and massive stars have a convective core which real extension is not really known. Indeed the turbulent eddies do not stop at the radius given by the Schwarzschild criterium but penetrate in the adjacent convectively stable regions where they are decelerated.

It is important to include this extension in stellar modelling as the nuclear fuel, hence the evolution and the stellar parameters are modified. This can have important consequences in studies of age - abundances relations in chemical evolution of galaxies; in extragalactic studies based on massive stars which have convective core and rotate rapidely. This has also consequences on the relation mass-luminosity for Cepheids for instance which serve as distance indicators.

The mixing length is not able to predict such an extension; it has been empirically determined by comparison with observations. It is expected that Corot will provide, at least for a few specific stars, information on the rotation and rapid variation of the sound speed near the convective core of intermediate mass and more massive stars. This will give us some quantitative information on the extension of the central mixed regions.

Intermediate and massive stars rotate rapidely. From ground, spectroscopic determinations of the projected rotational velocity $v \sin i$ for a large set of A-B stars have been obtained (Royer et al 2000, 2002). Histograms of $v \sin i$ show that the bulk of A, B stars have velocity around 100 km/s with a decreasing tail which extends up to $v \sin i$ 300 km/s i.e. near break up velocity (Fig.2). It is expected that the interaction between convection and rotation modifies the penetration of the eddies in the overlaying radiative layers. This has been studied with 3D numerical simulations of a rotating spherical shell which is a simplified representation of a rotating convective core for a A type star and a rotation rate of 1/10 t 4 times the solar rotation rate $\Omega_\odot = 2.6\mu$Hz (Browning et al 2004). Fig.5 shows that indeed rotation strongly influences the convective motions which in turn redistribute angular momentum. The rotation is differential both in latitude and in radius in a rotating convective core. Sizes of ascending and descending flows are similar as the density contrast is small (only 2-3) unlike the case of the solar outer convective region. Convective motions overshoot into the radiative region above, which makes it oblate (prolate ie aligned with the rotation axis). The extension of overshooting appears to vary with latitude creating asymetries in the extent of the penetration. In average however, the entire mixed central region seems to remain spherically symmetric. For this simulation $r_{Sch} = 0.14R$ and $r_{ov} = 0.16R$, R is the stellar radius i.e. with an extension into the stable layers of about $0.02R = 0.2H_p$.

This is in agreement with empirical determination for these types of stars by fitting the main sequence turn off and isochrones. It is important to note that when rotation is increased, the mixed central region gets larger. As this extension depends on the rotation of the star, it can vary from one type of star to another, and even from one star to another.

Browning et al explain that overshoot extension depends on the stiffness of the entropy gradient. In case of a weaker stiffness, the penetration extends further into the radiative part. Increasing Ω without altering the viscosity results in a more laminar convection due to the stabilizing effect of the rotation and therefore to a greater overshooting: rotation seems to enhance overshooting. The authors caution that due to various simplifications of the physical description, extention of overshoot is likely to be somewhat overestimated .

In a recent paper, Brun et al. 2005 have modelled the convective core of a magnetized A star. They found that the differential rotation when Lorentz forces are accounted for in the redistribution of the angular momentum is greatly reduced and becomes much more time dependent. However their results indicate that the inclusion of magnetic effect does not seem to modify the amount of overshooting.

3.2. Transport of angular momentum in radiative regions

Another piece of information we are expected is the location and the magnitude of rotation gradient within the star, and particularly in radiative regions of solar like stars as this would allow testing various transport mechanisms of angular momentum and associated chemical mixing.

Stellar rotation profile results from angular momentum transport that-is the angular momentum redistribution from one region of the star to another which can have several origins:

• caused by evolution: expansions and contractions of stellar regions

• caused by hydrodynamical processes. In radiative regions, (differential) rotation causes large scale motions, i.e. meridional circulation, and hydrodynamical instabilities which generate turbulence which in turn contribute to the redistribution of angular momentum. In convective region, interaction between large scale convective motions and rotation is quite efficient in transporting angular momentum and generating differential rotation.

• caused by surface losses by stellar winds (dynamo, thermal radiative) or surface gain from surrounding (accretion)

• magnetic field or internal waves (Mathis, Zahn, 2005; Talon et al 2002; Talon 2006)

In radiative regions, turbulence is expected to be highly anisotropic due to vertical stratification which acts as a stabilizing agent. As a result, it can be reasonably assuned that the rotation is shellular ($\Omega = \Omega(r)$) which enables a 1D description. The radial transport of specific angular momentum in the shellular assumption is then governed by the equation (Zahn, 1992):

$$\rho \frac{d}{dt}\Big(r^2\Omega_r\Big)_{m_r} = \frac{1}{5r^2}\frac{\partial}{\partial r}\Big(\rho r^4 U(r)\ \Omega_r\Big) + \frac{1}{r^2}\frac{\partial}{\partial r}\Big(\rho r^4\ D_v\ \frac{\partial \Omega_r}{\partial r}\Big) \qquad (1)$$

where $\Omega(r)$ is the rotation rate of the assumed shellular rotation; $U(r)$ is the velocity of the meridional circulation. The description is lagrangienne with $dm_r = 4\pi\rho r^2 dr$ and m_r the mass enclosed in a sphere of radius r, hence expansion and contraction effects are automatically taken into account. The first term on the right hand side is advection by meridional circulation and the second term is diffusion by weak vertical turbulence (Zahn, 1992; Maeder, Zahn 1998). Turbulence here is assumed driven by shear due to differential rotation (vertical shear $\Omega(r)$). Onset for turbulence occurs only if the flow satisfies a criterium (modified Richardson) which is still debated as it must include various stabilizing and destabilizing processes (μ gradient- radiative diffusion...). Horizontal shear $\Omega(\theta)$ acts to suppress the instability. Due to a vertical stable stratification, turbulence is highly anisotropic and horizontal turbulence is much more efficient in homogeneize the meddium hence turbulent transport coefficient must satisfy $D_h >> D_v$.

These processes cause chemical transport (directely or indirectly) which in turn affects the structure and the evolution of the star. Transport of chemical elements is given by the equation :

$$\rho\Big(\frac{dc_i}{dt}\Big)_{m_r} + \frac{1}{r^2}\frac{\partial \rho r^2\ c_i U_i^{diff}}{\partial r} = \frac{1}{r^2}\frac{\partial}{\partial r}\Big(\rho r^2\ (D_v + D_{eff})\ \frac{\partial c_i}{\partial r}\Big) \qquad (2)$$

where c_i is the concentration and U_i^{diff} the microscopic diffusion velocity of the chemical element i. The second term on the left hand side represents effect of atomic diffusion. The two terms on the right hand side model effect of rotationally induced transport.

While the assumption of strong anisotropic turbulence generating a shellular rotation profile $\Omega(r)$ likely holds true, the difficulties lie in determining the expressions of the turbulent diffusion coefficients

D_v, D_h, D_{eff} in Eq.1, Eq.2 and establishing a realistic criterium for the onset of turbulence in radiative regions (Zahn, 1992; Maeder, 2003; Mathis, et al 2004). These are still uncertain, advances are based on results of numerical 3D calculations (Browning et al. 2004) or laboratory experiments and could well afford information and observational constraints as Corot precisely could bring up.

Two types of rotationally induced processes of mixing have been identified: *mixing of type I* where both angular momentum and chemical elements are transported by rotationally induced mechanisms and *mixing of type II* where again chemical elements are transported by rotationally induced processes but for transport of angular momentum, other processes are more efficiently operating: internal gravity waves and/or magnetic field). Effect of rotation in transporting angular momentum here arises through Coriolis force which causes different behavior (in particular damping properties) between prograde et retrograde waves and therefore a net non zero momentum flux (Mathis 2004, phD).

The circulation is driven by gain or loss of angular momentum in surface. Hence if in absence of angular momentum loss, there is no need to transport angular momentum and the circulation remains weak: this happens to be the case for normal A type stars. On the other hand, important losses of angular momentum from the surface through a wind forces the need for a strong circulation in order to transport angular momentum to the surface. As far efficiency of transport of angular momentum in radiative regions is concerned which is responsible for uniform or nonuniform rotation profiles, we must therefore consider several cases of single stars (binarity is another issue not discussed here) according to their internal structure which itself depends on mass and age (Fig.6):

• Main sequence stars

- Low mass stars ($M \leq 1.4 M_{\odot}$) have an extended outer convective region which lose angular momentum through a dynamo driven wind (F-G-K stars) during their main sequence life time. The inner part is entirely radiative or for the most massive ones with a small convective core. By analogy with the Sun, we must expect a nearly uniform rotation profile in the inner radiative layer and latitudinal dependent rotation in the overlying convective region. As for the Sun, these stars have been speed down when evolving from their very youth and are much slower rotators than the intermediate mass stars. - Intermediate mass ($1.4 - 1.5 \leq M_{\odot} \leq 2.5 - 3 M_{\odot}$) are not expected to lose angular momentum nor mass as they have no extended external convective region for an efficient dynamo process and are too cool to have a radiatively driven wind. Because of evolution of the structure with expansion and contraction of mass shells, one expects that they rotate internally with a differential rotation profile ie radius dependence. We however ignore the stiffness of the rotation gradient.

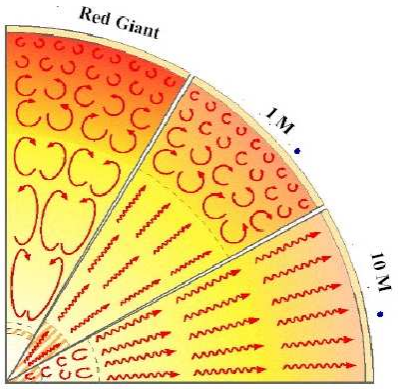

Figure 6. Structure (convective (circled arrows)/radiative (straight arrows) regions) of a star depending on its mass or age, whether it is a main sequence low mass star (right), an intermediate mass, main sequence star (middle) or a giant star (left)

- massive stars ($M_{\odot} > 3 M_{\odot}$ which lose mass through a radiatively driven wind (O-B stars). This mass loss (onset, magnitude, geometry) is strongly affected by rotation (Meynet & Maeder 2004; Maeder, 2006)

For massive and intermediate mass main sequence stars, rotationally induced mixing of type I has been found quite successful in reproducing observation (Talon & Zahn 1997; Maeder & Meynet 2000).

However for late type stars, this processus predicts a too fast rotating core for the Sun which seems to be in disagreement with heliosesimology (Matias & Zahn, 1998). Fig.7 shows results of calculations by Charbonnel, Talon (2005) : the rotation profile in the solar radiative region obtained from a 1D stellar assuming mixing of type I; the rotation if far from uniformity. When the rotation profile in the solar radiative region is obtained from a 1D stellar by assuming mixing of type II that-is including all transport processes of type I and including internal gravity wave transport but no for magnetic field, the redistribution of angular momentum is efficient enough to enforce uniform rotation in the radiative region of the Sun as observed by helioseismology. In addition, the observed behavior of the surface lithium abundance in function of the effective temperature of the star (L_i gap) is now reproduced by these models (Talon, Charbonnel 1998, 2003; Talon, 2006).

• Evolved stars: rotation on main sequence has a strong influence on the evolution of the structure and surface abundances in later stages when the star becomes a red giant

• PMS stars ;

Their fast rotation provides the initial condition for evolution of rotation on the main sequence.

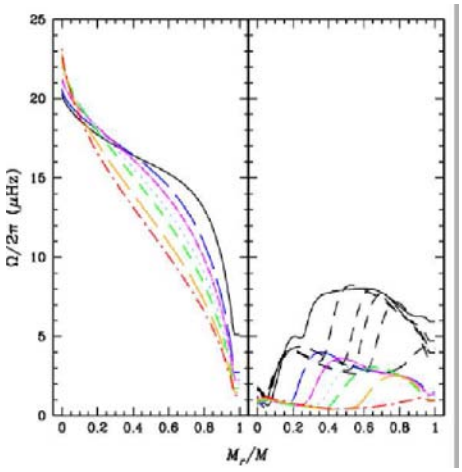

Figure 7. **top:** *Rotation profile in the solar radiative region obtained from a 1D stellar model assuming mixing of type I.* **bottom:** *rotation profile in the solar radiative region obtained from a 1D stellar model assuming mixing of type II (Zahn presentation 2005, AcRoCoRoT, taken from Charbonnel, Talon (2005)). Colors represent different ages.*

Part II Rotation and oscillations

It is expected that the space mission CoRoT (Baglin et al 1998) will measure oscillation frequencies with an accuracy of 0.5 μHz (20 days observation) and 0.08 μHz (150 days observations) for coherent modes ie self excited modes such as those of A-B type stars (δ Scuti, γ Dor, β Ceph)(Fig.8). For solar like stars, this will depend on the signal to noise ratio hence on the apparent magnitude of the star (see Goupil et al., this volume; Appourchaux et al HH exercises this volume).

These accurate measurements of the oscillation frequencies and the associated rotational splittings (Eq.5 below) will enable to infer information about depth and perhaps also latitude dependences of the internal rotation of a star. Forward techniques consist in comparing measured splittings with computed splittings assuming a rotation profile. Inversion techniques in principle do not assume a priori a rotation profile and determine either locally by suitable combinations of rotational splittings or globally by least squared fit minimisation its behavior with depth and latitude at least in regions where the modes associated with the detected frequencies propagate.

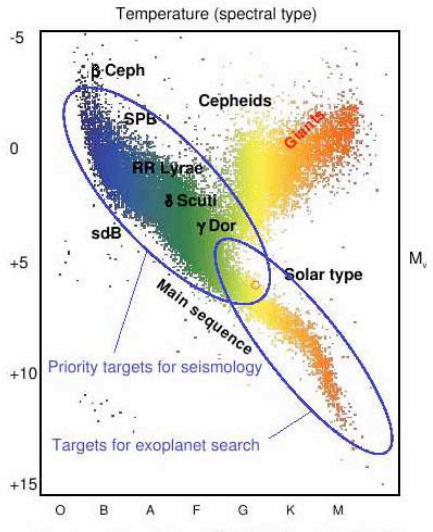

Figure 8. HR diagram showing several types of oscillating stars: two large classes are emphasized as special Corot target classes: intermediate mass A-B stars and solar like stars. A third class is now included in the favorite Corot target choices: red giants stars (diagram taken from Do Nascimento'stalk,2005 AcRotCoRoT, itself taken from Boisnard 2004, AcRotCoRoT)

3.3. Effects of rotation on oscillation frequency

Let $\nu_{0,n,\ell,m}$ be the frequency (in Hz) for a given oscillation mode when no rotation effect is included. The geometry of an oscillation mode is described by one single spherical harmonics, Y_ℓ^m, and the mode is $2\ell+1$ degenerate and the frequency is m independent $\nu_{0,m} \equiv \nu_0$ (Fig.9). When rotation is included, the centrifugal force distorts the structure of the star and therefore indirectly influences the wave propagation ie frequencies; on the other hand, Coriolis force has a direct effect on the wave propagation and on the oscillation frequencies. As a result, the symmetry breaking lifts the frequency degeneracy and the frequencies become m dependent. For symmetry reasons, it is usually assumed an axisymetric rotation $\Omega(r,\theta)$. The equilibrium structure then remains axisymetric; the modes can be labelled with a well defined azimuthal indice m.

The eigenmodes are computed using a basis which must be appropriately chosen in case of rapid rotation (Lignières et al 2006, Reese et al 2006) and which reduces to the usual vectors in spherical coordinates when rotation is slow enough to authorize perturbation expansion as in Sect.3.3.1 below.

For later discussions, it is convenient to distinguish between *fast, moderate and slow* rotation classified

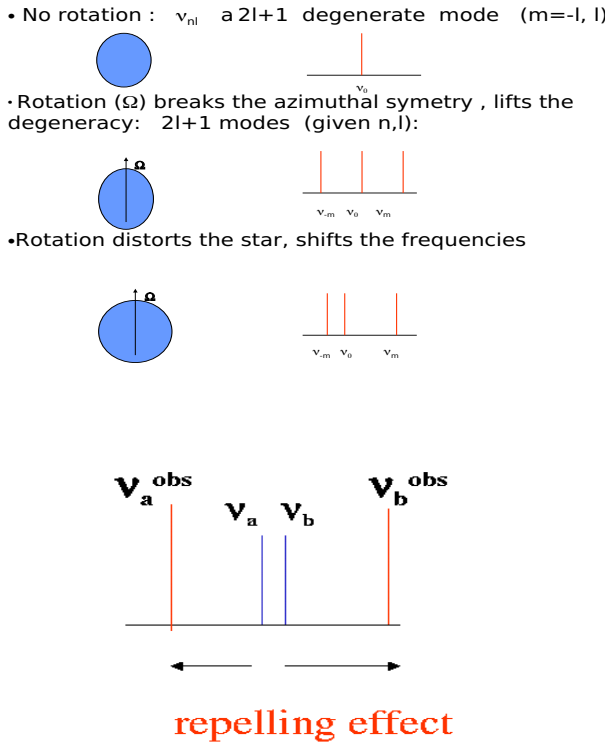

Figure 9. Schematic representation of effects of rotation on oscillation frequencies. From top to bottom, a degenerate mode n, ℓ in absence of rotation; a multiplet when rotation lifts the m degeneracy: first order effect due to Coriolis force gives rise to an equally spaced multiplet; the equla spacing is destroyed by second order effects mainly due to centrifugal distorsion; finally corrections due to near-degeneracy must be applied to modes with degrees $\ell, \ell+2$ and same azimuthal indice m. Correcting for near degeneracy results most often in repelling the close (ie near degenerate) frequencies

according to two parameters:

$$\epsilon = \Omega^2/(GM/R^3) \qquad \mu = \Omega/\omega \qquad (3)$$

where ϵ represents the centrifugal over gravitational strengths and μ compares the rotation time scale (Coriolis force) compared to the oscillation period. Then

• **slow** rotation here means $\epsilon, \mu << 1$ and first order perturbation in Ω is enough.

• **moderate** $= \epsilon, \mu \sim< \epsilon_{max}, \mu_{max}$ rotation is included as a perturbation but higher order $(O(\Omega^2), O(\Omega^3)$ contributions must necessarily be included in order to represent correctly the frequency spectrum.

• **fast** : $\epsilon, \mu > \epsilon_{max}, \mu_{max}$ 2D equilibrium models and non perturbative approach for computing the oscillation frequencies are required.

The upper limits $\epsilon_{max}, \mu_{max}$ depend on the star as it depends on the frequency range of its excited modes. More rigorously speaking, perturbation methods cease to be valid whenever the wavelength of the mode reaches the order of $\sim \epsilon R$ where R is the stellar radius that-is for p-modes with high enough frequencies or g-modes with low enough frequencies

3.3.1. Effect of rotation as a perturbation on oscillation frequencies

We focuse here on spheroidal modes only and we consider only the depth dependence of rotation hence $\Omega(r) =< \Omega(r,\theta) >_{horizontal}$. When rotation is slow enough, ϵ and/or μ are small and perturbation methods can be used. However, with increasing rotation rates, one must includes higher and higner order corrections to the frequency for a given accuracy (such as Corot frequency measurement accuracy)

• Slow rotators ; $O(\Omega)$

Slow rotation, as in the solar case for instance, can be treated as a perturbation and only the first order correction (from Coriolis force) is retained. Oscillation frequencies then are given by

$$\nu_{n,\ell,m} = \nu_{0,n,\ell} + m\frac{\Omega_s}{2\pi}(C_{n,\ell} - 1) \qquad (4)$$

in an inertial frame, with Ω_s is the surface rotation rate (in rad/s) and and $C_{n,\ell}$ is the Ledoux constant (DG92).

One defines the linear and the generalized rotational splittings respectively as:

$$\delta_{0,m} = \frac{\nu_{n,\ell,m} - \nu_{0,n\ell,m}}{m} \qquad \delta_m = \frac{\nu_{n,\ell,m} - \nu_{n,\ell,-m}}{2m} \qquad (5)$$

When Ω is uniform, then $\delta_m/(C_{n,\ell} - 1) = \Omega$ is a constant with $C_{n,\ell} = \frac{1}{I}\int K(r)dr$. Eq.5 is an integral equation for a shellular rotation rate as

$$\nu_{n,\ell,m} = \nu_{0,n,\ell} + m\frac{\Omega_s}{2\pi}\int_0^R K(r)\frac{\Omega}{\Omega_s}dr \qquad (6)$$

where the kernel $K(r)$ depends on the eigenmode, r is the radius. This relation can be inverted to yield $\Omega(r)$.

• For moderate rotation, $O(\Omega^2, \Omega^3)$

For moderate rotation, one has to take into account higher order (second and third order) corrections. Several degrees of approximation for realistic models have been studied over the years (Dziembowski, Goode (1992, DG92), Soufi et al 1998(SGD98), Suarez et al 2006, Karami et al 2005)

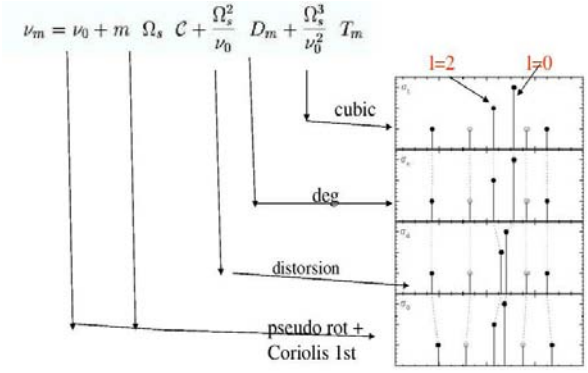

Figure 10. Oscillation frequencies corrected for rotation effects for two modes which are a $\ell = 0$ and $\ell = 2$ modes when no rotation is included. The model is a 1.8 $M_\odot$. Rotation included as a perturbation. A uniform rotation rate is assumed with v= 93 km/s. From bottom to top, successive higher order corrections are added to the zeroth order frequency (bottom) to provide the final correct frequency up to 3rd order (top) (from Goupil et al. 1999)

Oscillation frequencies must then be corrected according to

$$\nu_{n,\ell,m} = \nu_{0,n,\ell} + m\frac{\Omega_s}{2\pi}(C_{n,\ell} - 1) + \frac{\Omega_s^2}{2\pi\omega_0}\ D_{n,\ell,m} + \frac{\Omega_s^3}{2\pi\omega_0^2}\ m\ T_{n,\ell,m} \quad (7)$$

where $\omega_0 = 2\pi\nu_{0,n,\ell}$ and $C_{n,\ell}$ is the Ledoux constant Expressions for the $D_{n,\ell,m}, T_{n,\ell,m}$ coefficients (SGD98) show that they verify $D_{n,\ell,m} = D_{n,\ell,-m}$ and $T_{n,\ell,m} = T_{n,\ell,-m}$ which indeed is a general property resulting from the symmetry between a star and its mirror image with respect to any meridional plane as demonstrated by Reese et al. (2006).

The 'zeroth order' frequency ν_0 in Eq.7 actually includes the effect of the centrifugal force average over the surface (spherically symmetric distorsion) through an effective gravity g_{eff}; It does also includes some contribution of Coriolis force (if derived as in SGD98) and strictly speaking is m dependent. This dependence is omitted here for sake of clarity. The second term is the first order (Coriolis) correction and the last two terms represent effects of nonspherical distorsion of the star on the oscillation and third order correcton due to both centrifugal and Coriolis forces.

At 2nd order ($O(\Omega^2)$) the centrifugal force in distorting the shape of the star is responsible for the fact that a pure radial mode, for instance, of a nonrotating star can no longer exist when the star rotates. If rotation is low enough, the mode can keep its main nature as radial but with a contamination from other even ℓ modes. The contamination by the $\ell = 2$ mode mainly depends on the ratio of the inertia of both modes. Conversely the mode $\ell = 2$ is also contaminated by the radial mode. This happens when frequencies of both modes are close to each other. More generally, for large rotation, the modes can no longer be described with a single spherical harmonics. An effect which we refer to as *near degeneracy*. This is taken into account in writing that the mode is in fact a linear combination of two modes a and b which satisfy the conditions: $\ell_b = \ell_a + 2, m_a = m_b, \omega_a \sim \omega_b$

Let two modes labelled a and b with $\delta = \nu_a - \nu_b \sim 0$ then mode a is contaminated by mode b ie ν_a^{obs} ; mode b is contaminated by mode a ie ν_b^{obs} then their frequencies are given by :

$$\nu_a^{obs} = \bar{\nu} - \tfrac{1}{2}\sqrt{\delta_{ab}^2 + H_{ab}^2} \quad (8)$$

$$\nu_b^{obs} = \bar{\nu} + \tfrac{1}{2}\sqrt{\delta_{ab}^2 + H_{ab}^2} \quad (9)$$

with $\bar{\nu} = (1/2)(\nu_a + \nu_b)$ is the mean frequency and $\delta = \nu_a - \nu_b$ is the small separation ; H_{ab} is a coupling coefficient (see DG92, SGD98, Goupil et al. 2000, 2002; Suarez et al 2006, Karami et al 2005)

Such near degenerate frequency corrections can reach the level of $0.5\% - 2\%$. This is illustrated in Part III.

3.3.2. Effects of fast rotation on oscillation frequencies

For rapidly rotating stars, a perturbative approach is no longer applicable. One must turn to a 2D numerical approach to compute both the equilibrium model and the eigenmodes. Lignières et al. (2006) and Reese et al. (2006) have built a 2D numerical technique to compute nonperturbative oscillation frequencies. The solution is searched for as a summation over the spherical harmonics (up to $\ell = 80$ in Eq.4) for the angular dependence and decomposed over Chebyshev polynonials for the radial dependence of the eigenmodes. The equilibrium model in these studies is a self-gravitating uniformly rotating polytrope of indice 3 with rotation taken in a range from 0 to 0.59 Ω_K where Ω_K is the break up velocity $\Omega_K = \sqrt{GM/R_e^3}$ with R_e the equatorial radius. Investigation concerned first the effect of the centrifugal force alone (Lignières et al 2006) then both the centrifugal and Coriolis forces were included (Reese et al 2006). For details concerning the adopted numerical techniques, see Lignieres et al. (2006), Reese et al. (2006) and references therein. These authors have then studied the properties of p-modes in the frequency range of δ Scuti stars. A brief summary of some of their results is given in Sect.6 below.

When the star is non rotating, modes are easily classified as one assigns a single spherical harmonics with one given ℓ. When the star is rapidly rotating and the mode structure is given by a sum of many spherical harmonics, it is more difficult to classify the

modes, especially when they are involved in avoided crossings. In order to adress this difficulty, Lignières et al. (2006) followed several modes from zero rotation to 0.59 Ω_k. They found that even at fast rotation rates, it is still possible to classify the modes and assign them a ℓ value, based on the correspondance with modes in a non-rotating star.

Part III A-B type stars

Corot in its SISMO field will observe A-B stars such as β Cep (B type, ie massive main sequence stars), δ Scuti and γ Dor stars (A, intermediate mass main sequence stars) (Fig.8). Results from seismology from ground are still very sparse for these stars but seem to confirm the fact that the central regions of A-B stars rotate at least 2 or 3 times faster than their surface layers.

δ Scuti stars (PMS, MS post MS) have projected rotational velocities in the range $v \sin i = 70{-}250 km/s$ (Fig.2). This identifies them as moderate to rapid rotators in a $\epsilon - \mu$ diagram (Fig.24). For these stars, rotation strongly affects the location in HR diagram, the mode visibility and identification, mode excitation and selection (for a review, see Goupil et al. 2004 and references therein).

β Cephei stars are more massive stars. Their rotations are slow or moderate and they have no convective envelope, which makes their modelling easier. Two stars illustrate well the success found in their seismic modelling: HD 129929 (Aerts et al. 2004, Dupret et al 2004) and ν Eri (Pamyatnykh et al. 2004, Ausseloos et al. 2004). These two stars have well identified pulsation modes (at least 8 for ν Eri and 6 for HD 129929). Their seismic analyses give strong constrains on the location of the convective core boundary and overshooting parameter $d_{ov} \simeq 0.1$ in one case and $d_{ov} \simeq 0.3$ for the other one. In each of these stars, 2 rotational multiplet structures are clearly identified. Their interpretation allows the determination of their internal rotation compared to the surface. In both cases, the core rotates about 3-3.5 faster than the surface. Many more modes (higher degrees, more multiplets) are expected to be observed in the β Cep stars observed with COROT.

γ Dor stars are g-modes pulsators. The excitation of their modes is well explained by non-adiabatic models (Dupret et al. 2005). Their long periods (0.3 to 3 days) are of the same order as the rotation ones. Hence, rotation is expected to affect strongly the frequency pattern of these stars (Dintrans & Rieutord, 2000). As for δ Scuti and β Cephei stars, without mode identification based on other observables than frequencies, no unique solution is found. Taking accurately the effect of rotation into account is the next step for feasible seismic studies of γ Dor stars.

4. EFFECT OF ROTATION ON THE STRUCTURE AND EVOLUTION OF A-B TYPE STARS

Talon, Zahn (1997) studied the effects of transport of internal stellar angular momentum and induced transport of chemical elements on the evolutionary track and structure of a $9M_\odot$ model according to Eq.1, Eq.2 above with D_v, D_h, D_{eff} coefficients given by Zahn (1992). Following this study, several works such as Meynet & Maeder (2000) investigate consequences of rotationally induced transport in massive stars on their structure, evolution and interaction with their environments (mass loss, yields). For a review see Meynet, Maeder (2004).

Using the same evolutionary code with the same assumptions as in Talon, Zahn (1997), calculations for less massive models showed how rotationally induced transport affects the evolutionary track of a $\sim 1.75M_\odot$ model (Goupil, Talon 2002). Four types of models were built assuming 1) no rotation, no overshoot - 2) no rotation, overshoot included with a classical value for the overshoot extension $d_{ov} = 0.2H_p$ with H_p the pressure scale height. - 3) No overshoot but rotationally induced transport assuming a rotational velocity of $v = 70,100$ km/s. The corresponding evolutionary tracks are shown in Fig.11. As no mass and angular momentun losses are included, no net torque is applied at the surface of the star, hence total angular momentun is conserved. In that case, only a weak circulation is taking place. It is however able to transport inward enough hydrogen to increase the main sequence track as does the overshoot although with a quite different result in the evolution in the vicinity of the TAMS.

Models were then chosen to represent the δ Scuti star FG Vir with masses adapted to keep the models at the same location in the HR diagram. The structures of these models, as represented in Fig.11 by the Brunt-Vaissala frequency N. Although the evolution of a rotating model in the HR diagram is close to that of a nonrotating model with overshoot, the Brunt-Vaissala frequency inner maximum remains close to the one of the model without overshoot nor rotation. This can have important consequences on the frequencies of g and mixed modes which are sensitive to the properties of those inner regions for such a star. Fig.11 also shows the rotation profiles of the rotating models. The ratios Ω_c/Ω_{surf} differ by 14% between the two models which is enough to modify significantly the oscillation frequencies of modes which have significant amplitudes in the vicinity of the rotation gradient.

As mentionned earlier, uncertainties remain in the expressions for the transport coefficients (mainly D_h) as well as for the criterium for the onset of turbulence. Several works adressed these issues and gave rise to different forms for these coefficients and cri-

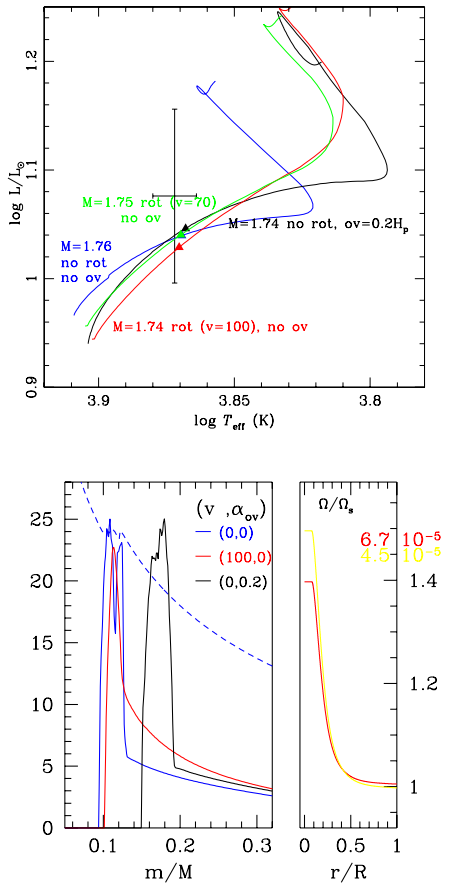

Figure 11. **Top:** *Evolutionary tracks in a HR diagram for evolution of models (representative of FG Vir): standard models i.e without rotation with no core overshoot (blue curve) and including core overshoot ($0.2H_p$) (black curve); models including rotationally induced mixing, no overshoot (surface rotational velocity $v = 100km/s$ (red curve) and $v = 70km/s$ (green curve) at the stage labelled with a triangle).* **bottom left:** *Inner maximum of the Brunt-Vaissala frequency for the selected models shown with triangles on the top pannel with the same line styles.* **bottom right:** *rotation rate normamized to a surface value corresponding to $v = 100km/s$ (red curve) and to $v = 70km/s$ (yellow curve). (from Goupil, Talon 2002)*

terium (Mathis et al. 2004 and references therein). Mathis et al. (2004) studied the effect of enhancing the horizontal turbulent transport on the evolution of 1.5 Msol models compared to previous calculations. This results in increasing the vertical transport and mixing of chemical elements.

In view of future applications to Corot target stars, rotationally induced transport according to Eq.1 and Eq.2 has also been recently implemented in the evolutionary code Cesam assuming transport coefficients given in Mathis & Zahn (2004). Moya et al (2006) computed evolutionary tracks for $1.5M_\odot$ models assuming no overshoot but different other types of transport: 1) atomic diffusion alone 2) uniform rotation alone (assuming conservation of total angular momentum with evolution) 3) rotationally induced mixing following the approach of Mathis & Zahn (2004) 4) same as 3) with atomic diffusion included

Fig.12 shows that the tracks are not significantly modified at the beginning of the main sequence. The authors then selected models which fall very close to each other in an observational box (with classical uncertainties on the effective temperature and luminosity). Important differences betwen these models can be seen on the hydrogen profile for instance (Fig.12). Atomic diffusion significantly modifies the H abundance in surface (Morel, Thevenin 2002) compared to the H abundance in absence of atomic diffusion. In turn, rotationally induced transport which is important in the surface layers smoothens the effects of atomic diffusion and decreases back the hydrogen abundance. We expect from these structural differences large differences in the oscillation frequencies at 'zeroth order' level ($\nu_{0,n,\ell}$ in Eq. 7) for those modes which are sensitive to surface properties namely high frequency p-modes as seen in Fig.13. Relative differences between frequencies $\nu_{0,n\ell}$ of a reference model (ie without rotation nor atomic diffusion) and of models which include atomic and/or rotation are almost independent of the frequency except at low frequencies (mixed modes). Differences with frequencies of a model including only atomic diffusion amount to ~ 0.015 whereas differences are much larger when the model includes uniform rotation (with conservation of total angular momentum) with changes of about 5%. When effects of rotation are included, magnitude of the changes are in between at the level of 4%.

Finally comparisons between a (mid)main sequence model evolved from a homogeneous initial model and a (mid)main sequence model which is evolved with PMS calculation of models including rotation (Moya et al. 2006) show little differences in the evolutionary tracks and in the rotation profile. Again here we expect nevertheless significant differences in the oscillation frequencies.

These preliminary results must be taken with caution

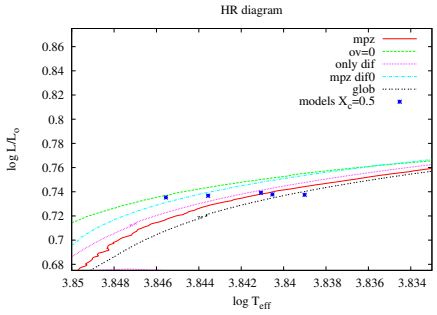

Figure 12. Evolutionary tracks of !.5 $M_\odot$ main sequence models in a HR diagram. Colors correspond to different assumptions about internal transport processes: all models are without overshoot. The track of standard models (ie with no rotation, no atomic diffusion) is represented in green; the track of models with diffusion only is pink; the black curve corresponds to models with atomic diffusion and uniform rotation with time independent total angular momentum; the red curve represents tracks for models with rotationally induced transport according to Mathis, Zahn, 2004 with atomic diffusion and and without atomic diffusion (light blue curve). (taken from Moya et al 2006)

as comparisons are presently being carried out with results from another evolutionary code (STAREVOLV) where rotationally induced transport has been already implemented and tested (Palacios et al. 2003). The comparison seems to indicate that our present implementation yields a too strong horizontal turbulent diffusion.

5. MODERATE ROTATORS: PERTURBATIVE APPROACH

Studies in this section concern modes with frequencies in the range where perturbation techniques are valid that-is low frequency p-modes and high frequency g-modes

For δ Scuti stars with $\epsilon = 0.014 - 0.14$ and $\mu = 0.01 - 0.2$ for instance, it is necessary to include $O(\Omega^2, \Omega^3)$ order corrections due to rotation when computing oscillation frequencies.

5.1. Moderate uniform rotation:

Using SGD98 approach, Goupil et al (1999) investigated the effects of a moderate rotation on the oscillation frequencies of a typical δ Scuti star model with $1.8 M_\odot$, $logT_{eff} = 3.876$, a photospheric radius of $2.125 R_\odot$ $v = 10$ to 100 km/s. From such a study, several conclusions were drawn:

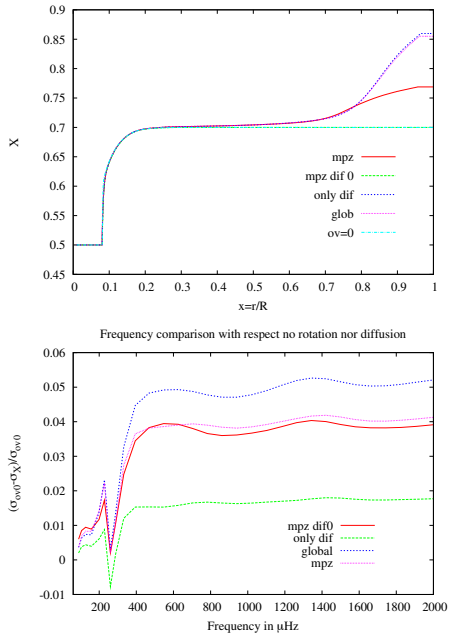

Figure 13. **top:** *Hydrogen profiles of $X_c = 0.5$ models of Fig.12.* **Bottom:** *Comparison between frequencies for $\ell = 2, m = 0$ modes computed for a reference model (assuming no rotation, no overshoot, no atomic diffusion) and frequencies of models computed with different assumptions about internal transport processes (from Moya et al 2006)*

The ratio $\mu^2/\epsilon^2 \sim 1 - 15$ rapidly decreases with increasing frequencies ($\sigma >> 1$) and distorsion due to the centrifugal force dominates over the Coriolis effect for high frequency p-modes while it is the opposite for low frequency g-modes.

The aspherical distorsion shifts all frequencies by a quantity $(\Omega_s^2/\omega_0) D_{n,\ell,m}$ which depend on m, ℓ for axisymmetric modes .

For high frequency p-modes, one can neglect effects of horizontal displacement in front of the vertical ones. Using this approximation in expressions for $D_{n,\ell,m}$ (which can be found in DG92, SGD8, Karami et al. 2005, Suarez et al. 2006), one finds

$$\frac{\Omega_s^2}{2\pi\omega_0}\ D_{n,\ell,m} \sim Q_{\ell,m}\ V_{n,\ell} \qquad (10)$$

where the geometrical factors are given by:

$$Q_{\ell,m} = \frac{\Lambda - 3m^2}{4\Lambda - 3} \qquad Q_{\ell,\ell+2,m} = \frac{3}{2}\ \beta_\ell\ \beta_{\ell+2} \qquad (11)$$

with

$$\Lambda = \ell(\ell+1) \qquad \beta_\ell = \left(\frac{\ell^2 - m^2}{4\ell^2 - 1}\right)^{1/2} \qquad (12)$$

The $V_{n,\ell}$ coefficient can be approximated as

$$V_{n,\ell} \sim \epsilon^2\ \omega_0\ \ < S_2 > \qquad (13)$$

where

$$< S_2 >= \frac{1}{I} \int_0^R y_n^2 \ (2r\frac{du_2}{dr} + u_2) \ \rho \ r^2 \ dr$$

with $y_{n,\ell}$ the relative fluid displacement eigenfunction in Eq.?? (defined as y_1 in Unno et al.1989). The quantity u_2 is related to the perturbation of the gravitational potential by rotation, $\phi_{22} \ u_2 = \phi_{22}/(r^2\Omega_s^2) + (1/3)(\Omega/\Omega_s)^2$. ϕ_{22} is defined by $\phi(r,\theta) = \phi(r) + \phi_{22}(r)P_2(\cos\theta)$ is solution of a perturbed Poisson equation, $P_2(\cos\theta)$ is the 2nd order Legendre polynomial (DG92, Soufi et al 98) The structural quantity $< S_2 >$ is nearly model independent ($\mathcal{D}/3$ of Fig.8 in Goupil et al. 1999).

For two degenerate modes labelled $a = (n,\ell)$ and $b = (n',\ell+2)$, one can assume $V_a \sim V_b \sim V_{ab}$ as $y_{n,\ell} \sim y_{n',\ell+2}$ in the outer parts which contribute most to V_{ab}. Hence one approximately has:

$$\mathcal{H}_{ab,m} \sim \mathcal{Q}_{\ell,\ell+2,m} V_a \qquad (14)$$

For high radial order modes, the coupling coefficient $H_{ab,m}$, like D_{nlm}, increases linearly with the frequency. Degenerate coupling is found to dominate for $v > 50km/s$.

A measure of the asymetry of a multiplet is given by:

$$\begin{aligned} \Delta\nu &= \nu_{n,\ell,m=0} - \tfrac{\nu_{n,\ell,m}+\nu_{n,\ell,-m}}{2} \\ &= -\nu_0\epsilon^2 \tfrac{6m^2}{4\Lambda-3} < S_2 > \end{aligned} \qquad (15)$$

The asymetry in the multiplet also increases linearly with the frequency ν_0 and the squared rotation rate Ω^2.

Cubic order effects are at the relative level of $10^{-2} - 10^{-3}$ that-is that they are non negligible at the level of Corot accuracy for moderate rotating δ Scuti stars and more important for non axisymmetric modes than centroid modes.

Using Eq.7 in Eq.5, the generalized splittings for non-degenerate modes take the form:

$$\delta_m = m\Omega_s(C_{n,\ell} - 1) + m\frac{\Omega_s^3}{\nu_0^2} \ T_{n,\ell,m} \qquad (16)$$

In absence of cubic effects, the ℓ quantities d_m, $(m = 1,\ell)$ such that

$$d_m = \frac{\delta_m}{(C_{n,\ell} - 1)} \qquad (17)$$

are the same and yield the true rotation rate. When cubic effects are nonnegligible, the correct rotation value cannot be recovered directly from Eq.17. However it is possible to combine the different values of d_m so as to eliminate the high order perturbations and to recover the rotation rate (Sect. 5.3 below).

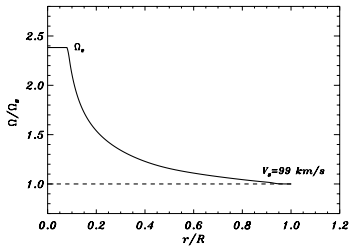

Figure 14. Rotation frequency through the star normalized to its surface value. The continuous line represent a shellular rotation profile and the dashed line to a uniform rotation profile. Models are built with the same surface rotation frequency $\Omega_S = 9.98\,\mu Hz$. Figure taken from Suarez et al. 2006.

For a given mode, avoided crossing, which is a signature of the inner gradient of Brunt-Vaissala frequency (due to μ gradients in the vicinity of a convective core), arises at cooler temperatures for rotating models than for no rotating models. of same mass and age (Goupil, Talon 2002).

Difficulties in identifying the modes of δ Scuti stars can be somewhat overcome in using histogram frequencies and statistical analyses, provided that a large number of modes are detected as expected with Corot data. However for moderate and fast rotating stars, histograms of frequencies are strongly affected by rotation as shown with the case of FG Vir and for high rotation rates the peaks representative of the rotation at low frequency is smeared out when v reaches 70-100 km/s (Goupil et al. 1999)

Finally frequencies of a given multiplet obey a near resonance of the type $\Delta\nu \sim 0$ (Eq.15). Such a resonance can be responsible for a nonlinear coupling which can cause the amplitudes of a given multiplet to be asymetric and enforces This effect seems to be distroyed for fast rotation and therefore would exist in a limited range of rotation rate; amplitudes then become time dependent over a time scale which can be much shorter that the Kelvin Helmoltz time. This is one of the important issues we expect Corot to provide clues about.

5.2. Shellular rotation

The effect of radial differential (shellular) rotation on adiabatic oscillation has been studied for intermediate-mass rotating stars (δ Scuti stars,γ Dor) in the framework of the preparation of the Corot mission (see CW4) (Suarez et al., 2006) for a typical δ Scuti star. Equilibrium models are built with the evolutionary code CESAM (Morel 1997). Rotation is included by considering an effective gravity modified by the effects of the centrifugal force.

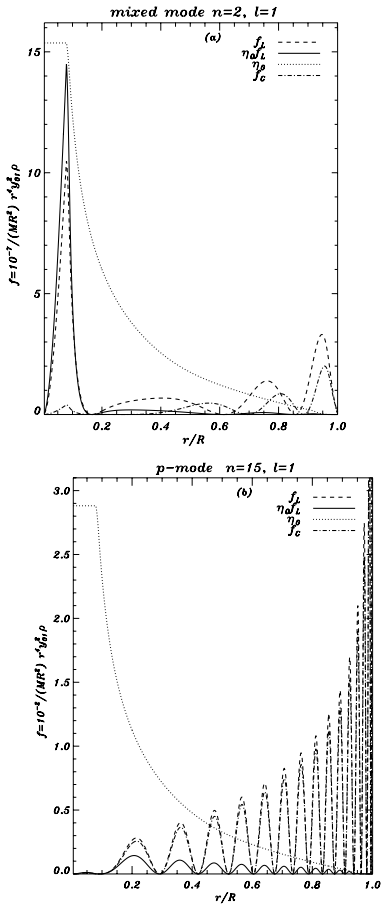

Figure 15. Weighted radial displacement eigenfunctions for a mixed mode (top) and a p mode (bottom) in function of the radial distance r (normalized to the radius of the star R). Solid and dashed lines represent the $f = \rho\, r^4\, y_{01}^2$ functions computed for a differentially rotating model with ρ the density. Dash-dotted lines represent the f function computed for a uniformly rotating model. Dotted lines represent the rotation profile given by the radial function $\eta_0(r)$ (the scale has been adapted for sake of clarity) (taken from Suarez et al. 2006)

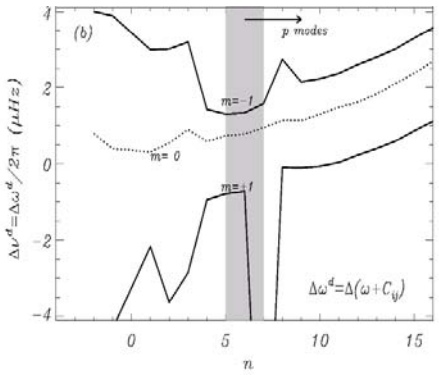

Figure 16. The plot displays mode-to-mode frequency differences between differentially and uniformly rotating $1.8 M_\odot$ models. Frequencies include near degeneracy corrections. Symmetric solid line branches represent from top to bottom, differences for $m = -1$ and $m = +1$ mode frequencies respectively. For $m = 0$ modes, differences are represented by a dotted line. In both panels, the shaded region represents an indicative frontier between the region of g and gp modes (left side) and p modes (right side). Figure taken from Suarez et al. (2006)

That is, only the spherically symmetric terms are considered. This is known by *pseudo-rotation* as is called in SGD98. Although the non-spherical component of the deformation of the star is not considered, its effects are included through a perturbation in the oscillation equations (Suarez, 2002 PhD). Rotationally-induced mixing and transport of angular momentum as described in previous sections are not included in the models used here. Two illustrative cases when prescribing the rotation profile $\Omega(r)$: 1) either instantaneous transport of angular momentum in the whole star (global conservation) which thus yields a uniform rotation, or, for sake of simplicity and illustrative purpose, 2) local conservation of the angular momentum (*shellular* rotation). In Fig. 14 both cases are depicted for two $1.8\,\mathrm{M}_\odot$ models with the same rotation velocity ($100\,\mathrm{km\,s^{-1}}$) at the stellar surface and very close in the HR diagram.

Adiabatic eigenfrequencies were computed following the perturbation formalism of DG92 and SGD98. up to second order in the rotation rate Ω allowing a radial dependence of $\Omega = \Omega(r)$. The effect of shellular rotation on the eigenfunctions is illustrated in Fig. 15, for a high radial order p mode (Fig. 15*b*) and for comparison in Fig. 15*a* for a *mixed* mode. As can be seen, for *gp* modes, the eigenfunctions present an inner maximum near the core $r/R \sim [0, 0.2]$. As the kinetic energy of these modes are large in core-close regions, large seismic differences between the uniform and the shellular rotation cases are reasonably expected. For high radial order p modes, *implicit* effects of shellular rotation on eigenfunctions are represented by dashed lines and can be compared to those

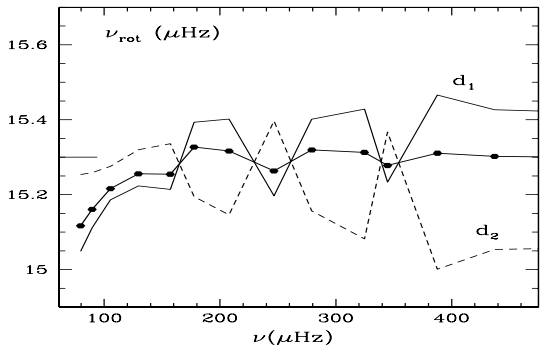

Figure 17. Recovering the rotation profile in the case of a moderately fast rotating $1.8M_\odot$ star. A uniform rotation has been assumed corresponding to a value 15.3 μHz (a rotational velocity of 144.5 km/s). The blue curves represent d_1 and d_2 (Eq.18) for $\ell = 2$ multiplets and the red curve is $d_1 + d_2/2$. The large excursion of d_1 and d_2 are due to the presence of mixed modes in this frequency range

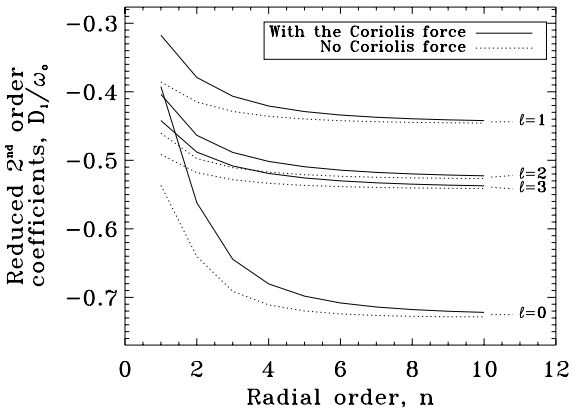

Figure 18. The reduced 2nd order coefficient D_1/ω_0 (Eq.19) decreases toward a constant with increasing radial order n for modes with different degree ℓ (solid line: Coriolis force is included; dashed line: Coriolis force is not included). At high frequency, as Coriolis effects are small and effects of the centrifugal force dominate, differences between both calculations are quite small. This is less true at lower frequency where Coriolis plays a nonnegligible role (taken from Reese et al. (2006)

for a uniform rotation. Maximum amplitudes of such modes are located near the stellar surface, where the eigenmodes do not differ much between the uniform and the shellular cases.

5.2.1. Effect of shellular rotation on the frequencies

Figure 16 displays $\ell = 1$ mode to mode frequency differences between frequencies computed assuming a uniform rotation and a shellular rotation (with a ratio $\Omega_{core}/\Omega_{surf} \sim 2$). Both models have the same surface rotation velocity $v = 100km/s$. Frequencies are computed according to (Eq.9). Differences can be larger than 1 μHz. Large effects due to near- degeneracy can be seen for *gp* modes, and for high-frequency *p* modes, which can reach up to 3 μHz. For the former modes, such effects are expected because the rotation profile rapidly varies in the inner layers at the edge of the convective core where *gp* modes have large amplitudes (see Fig. 15. For high-frequency *p* modes such effects can be explained by the structure spherical deformation caused by the centrifugal force, which mainly affects the zeroth-order oscillation frequencies. Indeed although high frequency p-modes have small amplitudes in the vicinity of the core, the rotation variation which is significant only in the vicinity of the core is felt by these modes strongly enough to modify significantly their frequencies. It is found that, although only a few triple-mode (or higher) interaction is present in moderately rotating δ Scuti stars the effect of taking such interaction into account instead of double interaction can be quite different depending on the configuration of the modes (closeness of the frequencies). We find that the effect can be occasionally amount up to a few μHz.

Hence, with such an accuracy, effects of shellular rotation are likely to detectable with Corot data, provided numerical eigenfrequencies reach this level of precision.

5.3. Recovering the rotation profile from moderately rotating star oscillation frequencies

As outlined by Dziembowski & Goupil (1998) and Goupil et al. (2004), it is possible to remove contaminations of high-order (second and higher) effects of rotation from the rotational splitting in order to recover the true rotation profile. Using Eq.16, splittings with different m are combined in order to eliminate cubic order pollution and to recover the rotation profile. Goupil, Talon (2002) illustrate the case with a $1.8M_\odot$ model with a uniform rotation corresponding to 15.3 μHz. The plot shows the behavior of frequency difference d_m (Eq.17 above) for $m = 1$ and $m = 2$ $\ell = 2$ modes in function of the associated $m = 0$ mode. The red curve $\delta_1 + \delta_2/2$ is found to be nearly uniform and give the value of the input uniform rotation rate. This will be efficient for modes which exist in nearly uniform rotating regions.

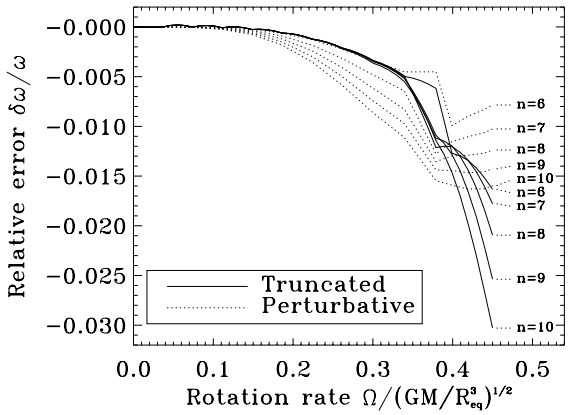

Figure 19. Relative differences between nonperturbative frequencies and perturbative frequencies computed according to Eq.19 for modes with radial order $n = 6, 10$ (dotted lines). Relative differences between nonperturbative frequencies and frequencies computed using a truncated formulation involving 2 poloidal and 2 toroidal modes (solid lines). These relative differences are plotted in function of increasing rotation rate Ω/Ω_K with Ω_K the break up rotation rate. from Reese et al 2006

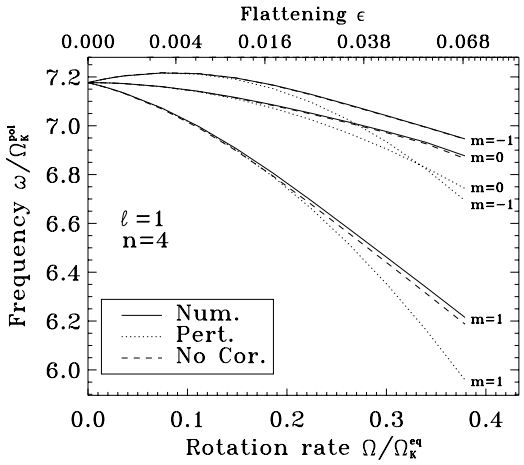

Figure 20. Evolution of the structure of a given multiplet (here $\ell = 1, n = 4$) when rotation is increased. For $\omega/\Omega_K > 0.2$, the differences $\delta\omega$ is larger than the value of the splitting itself and the $m \neq 0$ are not affecetd the same way. (from Reese et al. (2006))

In case of non uniform rotation or when the rotation is fast enough that all modes are degenerate, it is more difficult to remove high order perturbative effects of rotation and it is likely that one will have to use some a priori simplified rotation profiles or some iterative processes based on

$$\delta_m = \int_0^R dr K_1(r)\ \Omega(r) + \int_0^R K_2(r)\Omega^3(r) \quad (18)$$

6. RAPID ROTATION : NON PERTURBATIVE APPROACH

As already mentioned, Lignières et al. (2006) and Reese et al. (2006) have studied the effects of fast rotation for a self-gravitating uniformly rotating polytrope of index 3 with a rotation rate taken in a range from 0 to 0.59 Ω_K ($\epsilon = 0$ to 0.35)

6.1. Effets of the centrifugal force

The centrifugal force induces a decrease of the frequency because a rotating star has a larger volume and a smaller sound speed. As found by Lignières et al (2006), this decrease is in average proportional to the frequency, the rate of decrease being close to that of the mean density. Nevertheless, besides this average behavior, the frequency decrease is ℓ and n dependent and this differential effect modifies the structure of the frequency spectrum. It follows that the structure of a non-rotating frequency spectrum is destroyed. In particular, the small difference $\nu_{n,\ell} - \nu_{n-1,\ell+2}$ is no longer small above a certain rotation rate. Actually this quantity befomes nearly constant and characterizes together with the large difference $\nu_{n,\ell} - \nu_{n-1,\ell}$ the new structure of the frequency spectrum at large rotation rates.

Rotation also affects the properties of mode visibility since the angular dependence is no longer given by a unique spherical harmonic (SGD98, Daszynska-Daszkiewicz et al., 2002). Lignières et al (2006) show that the amplitude of the low frequency p-modes progressively concentrates near the equator as rotation increases. This effect strongly modifies the variation of the disk-averaging factor with the degree of the mode. In a non rotating star, the cancellation between positive and negative surface perturbations results in a strong decrease of the disk-averaging factor with the degree number. This property does not hold in rapidly rotating stars where the equatorially concentrated modes have similar surface distribution.

6.2. *Comparison between full and perturbative calculations*

An important issue is to establish the domain of validity of perturbative calculations. Accordingly, Reese et al (2006) compared results from full 2D calculations and from perturbation calculations. The last ones were carried out assuming that frequencies

take the form

$$\omega_{n,\ell,m} = \omega_{0,n,\ell} + m\Omega(C_{n,\ell} - 1) + (D_1 + m^2 D_2)\Omega^2 + m(T_1 + m^2 T_2)\Omega^3 \quad (19)$$

with $\omega = 2\pi\nu$. The coefficients $D_1, D_2, ...$ were determined by a least squared fit from results of full 2 D calculations assuming low rotation rates. Including both the centrifugal and Coriolis force, Reese et al (2006) computed frequencies of $\ell = 0$ to 3 and radial order $n = 1$ to 10. The studied polytrope corresponds to a $1.9 M_\odot$ and a polar radius of 2.3 $R_\odot$ typical of a δ Scuti star. Fig.19 shows the relative differences $\delta\omega/\omega = \omega^{(full)} - \omega^{(pert,3)}/\omega$ in function of the rotation rate normalised to the break up rotation rate Ω_K. $\omega^{(full)}$ are frequencies obtained with a full 2D numerical calculation and $\omega^{pert,3}$ frequencies computed up to third order according to Eq.19 above. The differences are seen to increase with the rotation rate and the radial order. They are mainly due to the centrifugal force as, as mentionned earlier, Coriolis force has a negligible effect at high frequencies. The differences become quite significant when $\Omega/\Omega_K < 0.1$ ($\epsilon < 0.01$)

Here significant means larger than the measurement accuracy of rotational splittings expected with Corot data. The comparison shows that the full calculation is required for $vsini > 50 km/s$ for Corot 150 days accuracy.

Fig.20 shows the evolution of the structure of a given multiplet (here $\ell = 1, n = 4$) when rotation is increased. For $\omega/\Omega_K > 0.2$, the differences $\delta\omega$ are larger than the values of the splittings themselves. The m and $-m$ components are not affected the same way.

Fig.21 displays the frequencies computed when adding successively higher order corrections according to Eq.19. At zero rotation rate, the mode is m degenerate. At small rotation rates (first order correction in green) nice evenly-spaced multiplets can be seen. At higher rotation rates, multiplets stars to be no longer equally spaced and multiplets start to overlap (second order corrections in blue). At even higher rotation rates, the initial structures within the multiplets and between multiplets are lost (third order corrections in red; full nonperturbative calculations in black)

In Fig.19, black lines represent relative differences betwen frequencies computed with a full nonperturbative calculation (with $L_{max} \sim 80$ in Eq.**??**) and frequencies obtained when truncating the summation to $L_{max} = 2$ in Eq.**??** that is includind two poloidal and 2 toroidal contributions. The relative differences become significant for slightly larger rotation rates than when a simple perturbation expression, Eq.19, is assumed. For instance, a relative frequency difference of is reached for $\epsilon \sim 0.18$ when a

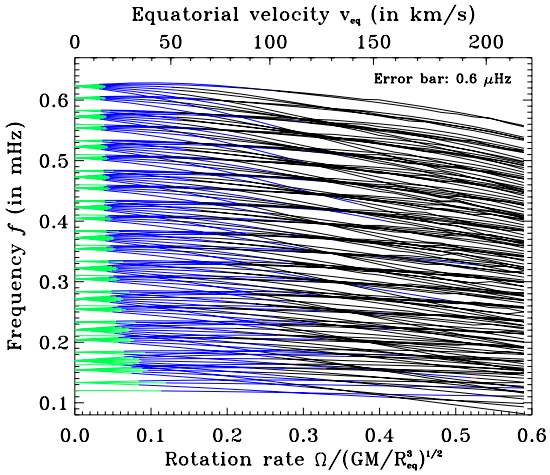

Figure 21. Plot of pulsation frequencies as a function of the rotation rate Ω/Ω_K. Modes have radial orders $n = 1$ to 10 and degrees $\ell = 0$ to 3, $m = -l$ to l. The top horizontal axis represents the flattening $1 - R_p/R_e$ where R_p is the polar radius and R_e the equatorial radius. Green curves indicate the domain of validity of 1st order perturbative calculations that-is allowing a 0.6 μHz differences (which corresponds to a Corot 20 day observing program) between nonperurbative and perturbative calculations . Blue (resp. red) curves indicate the domain of validity for 2nd order (resp.3rd order) perturbation calculations. Black curves corresponds to the nonperturbative frequencies. (from Reese, 2005 at 2nd Corot Brazil workshop)

perturbation (Eq.19) is assumed and for $\epsilon \sim 0.25$ when a truncated summation is used. To fix ideas however, for typical frequencies of excited modes of δ Scuti stars in the range $500 - 1000\mu$Hz a relative difference of 2.510^{-3} corresponds to a frequency difference of $1.25 - 2.5\mu$Hz significantly larger than the accuracy expected on splittings measurements with Corot data. Note that the truncated calculations correspond to pertubation calculations when systematically including near-degeneracy (Eq.9).

6.3. Conclusion

It is quite reassuring that a number of qualitative frequency characteristics found when using perturbation calculations subsist when rotation is real fast. Modes with a high radial order n are less affected by the Coriolis force than by the distorsion due to the centrifugal force is the main cause for deviations between frequencies in non-rotating stars, frequencies based on the perturbative approach and thise based on the non-perturbative approach.

Quantitatively, the non-perturbative approach tells us the limit of validity of perturbative methods. In the present case , the comparison with Corot measurement precision shows that perturbative results are no longer valid for $\Omega/\Omega_K > 0.2$ for radial order $n \sim 6$ and higher and for $\Omega/\Omega_K > 0.3$ for radial order $n \sim 1, 2$. For a rotation rate of $0.59\Omega_K$ (corresponding to a rotational velocity of 240 km/s for $1.8M_\odot, 2R_\odot$), the frequency spectrum stemmed from a nonperturbative calculation is very different than the frequency spectrum obtained from a perturbative calculation.

Finally, we list some Corot selected stars which are rotating fast and which quantitative seismic studies will require nonperturbative calculations.

Rapidly rotating primary targets for CoRoT		
Star identification	Stellar type	$v\sin i$ (in $\mathrm{km\,s^{-1}}$)
HD 181555	δ Scuti	170
HD 49434	γ Doradus	90
HD 171834	F3V	72

Some of CoRoT's rapidly rotating secondary targets		
Star identification	Stellar type	$v\sin i$ (in $\mathrm{km\,s^{-1}}$)
HD 170782	δ Scuti	198
HD 170699	δ Scuti	> 200
HD 177206	δ Scuti	> 200

The $v\sin i$ measurements are based on Poretti et al., 2005 and Corotsky.

Part IV Solar like oscillators : are they really slow rotators ?

Stars of spectral type F,G,K are usually considered as slow rotators. Custipoto et al. (2002, 2003) have determined values of $vsini$ of a large sample of F,G,K stars in the solar neighborhoud. The stars were selected specifically for their high $v \sin i$ values. Reiners & Schmid (2003) have also obtained values of $v \sin i$ for a sample of F-G-K type PMS and MS stars. These stars have often $v \sin i$ exceeding 15 km/s. As seen in Fig.1, for F,G,K stars, the bulk of stars is about 10 km/s- 15 km/s but the tail extends up to 30 km/s, the tail is more pronounced for K stars. These measurements show that solar like stars are slow rotators in comparison with more massive (A-B) stars but are often rotating more rapidely than the Sun.

Solar like oscillation high frequency p-modes are excited by stellar outer convective regions. For a growing number of solar like stars, high frequency p-modes have indeed been detected and in some cases with an enough large number of frequencies that the first seismic models have been built for $\alpha\ Cen\ A, B$, Procyon, η Boo (see references section). No splitting have been detected for solar like oscillating stars other than the Sun. We expect that some Corot target stars rotate fast enough that their rotational splittings will be detected, This means a $20-30$ km/s for a 1.5 $M_\odot$ (Goupil et al, this volume; Lochard et al 2005)

7. INFLUENCE OF ROTATION ON THE SMALL SEPARATIONS AND ECHELLE DIAGRAMS

Even though solar-like oscillators are considered as slow rotators, the $m = 0$ mode frequencies are affected by rotation for these stars (Goupil et al 2003). Lochard et al. (2006) show that the reppelling effect of near degeneracy (Fig.9) can significantly affect the frequency separation of modes ℓ and $\ell + 2$ with successive radial order as they have close frequencies which is referred to as *small separation*. This has been stressed by SGD98, Dziembowski (1997), Dziembowski, Goupil (1998). The small separation is often used to characterise the evolutionary stage (age) of the star. The small separations between $\ell = 0, 2$ and that between $\ell = 1, 3$ become so small that rotation, even at a modest rate of 15 km/s, leads to significant degeneracy effect.

The echelle diagram is useful to identify the ℓ value of modes associated with the detected frequencies. The echelle diagram is also affected by rotation to the same extent that the small separations are. This is illustrated in Fig.22 for 3 different values of the surface rotational velocity. Deviations from nonrotating model echelle diagram can be seen for $v > 25km/s$ particularly at high frequency. When only $m = 0$ modes are used, the effect is not large enough to lead to an error in mode identification. However deviations from echelle diagram for non rotating star must be taken into account when fits of the frequency curves in echelle diagram are determined in order to build a seimic models or when attributing the departure between observed and theoretical curves to a physical deficiency of the models such as turbulence in the outer layers (Straka et al. 2006).

At $v = 50km/s$ the effects are huge. However, the corresponding ϵ, μ tells us that the perturbation technique is probably no longer valid for computing the oscillation frequencies in that case and one must turn to techniques for rapid rotators (as mentionned Sect.6)

8. RECOVERING THE SMALL SEPARATION FREE FROM ROTATION CONTAMINATION

It possible to remove most of the contamination of higher order effects of the rotation for high frequency p-modes by combining suitably the splittings provided they are available. For solar like stars, rotation is indeed small enough that cubic order frequency corrections in Eq.7 are negligible. For high frequency p-modes, as is the case of solar like oscillations, the horizontal displacement is negligible in front of the vertical one. Using the approximate expressions for $D_{a,m}, D_{b,m}$ and $H_{ab,m}$ given in Eq. 10-14, it can be shown (Goupil et al. 2003) that the 'true' small separation $\delta_{n,\ell} \equiv \nu_a^{(\Omega=0)} - \nu_b^{(\Omega=0)}$ for $m = 0$ modes - that is the small separation free from rotation pollution - is given by

$$\delta_{n,\ell} \sim \left((\nu_a^{obs} - \nu_b^{obs})^2 - 4\ Q^2_{\ell,\ell+2,0} V_a^2\right)^{1/2} - (Q_{\ell,0} - Q_{\ell+2,0})\ V_a \qquad (20)$$

where the geometrical factors are given in Eq.11. Hence the small separation increases linearly with the frequency and with Ω^2.

The structure quantity $V_a \sim V_b$ itself can be obtained from the observed frequencies as

$$V_a = 3(s_{a,2} - s_{a,3})$$

with

$$s_{a,m} = \frac{1}{2}\left(\nu^{obs}_{a,m} + \nu^{obs}_{a,-m}\right)$$

for mode $a = (n+1, \ell = 3)$ and mode $b = (n, l = 1)$ for instance.

Note that we remove here the contamination of the frequency due to direct influence of rotation on the wave propagation hence the oscillation. The small separation still includes the indirect effect of rotation on the structure which is precisely what we want to probe. Also V_a is a measurable seismic quantity which can be inverted to provide information about the distorted structure.

Goupil et al (2003) condider the case of a $1.4 M_\odot$ with solar chemical composition, $\log T_{eff} = 3.810$ with rotation velocity $v = 10$ to 40 km/s (included for the spherical distorsion mean centrifugal force via an effective gravity). Modes are considered as systematically degenerate. Frequencies including rotation effects according to Eq.9 for modes $\ell = 0$ to 3 with radial order $n = 6 - 25$ have been computed. For this model, rotation increases the small separation by 1.2 μHz (Fig.23). From this value, one would then deduce that the star is younger than in reality by 1 Gyr when plotted in the mean small separation- mean large seperation diagram as proposed by Christensen-Dalsgaard (1993).

Fig.23 shows the small separations for modes $\ell = 1, 3$ computed without including rotation effects (= 'true' small separation) and including rotation effects for velocities 10,20,30 35 km/s respectively. Departure of the curves from the zero velocity one increases with the rotation rate Ω. From the 'polluted ' small separation $\nu^{(obs)} - \nu^{(obs)}$, one computes the 'true' small separation according to Eq.20. Fig.23 shows that the process is very efficient in recovering the small separation free of rotation effects.

9. CONCLUSIONS

If one compares with results of heliseismology, seismology of other stars has not yet been so successful except for white dwarfs and a few cases of main sequence stars. There are several reasons for this:

- Stellar parameters such as mass, age, chemical composition are not known with enough precision and must be considered as free parameters. These free parameters must be determined with enough precision on the basis of the seismic constraints. Only in that case, it can be possible to probe the internal physics of the star.
- For solar-like stars (α Cen, procyon, η Boo) there are still uncertainties on the frequency set and/or mode identification although they can be identified to some extent with techniques such as echelle diagrams. However the excited modes are low degree, high freauency that-is quite redondant.
- For stars other than solar like stars, excited modes are difficult to identify among the possible linearly unstable modes for a given star. Often, their mixed p-g nature and the effect of fast rotation complicate the frequency pattern.

Hence seismic studies for stars other than the Sun must be carried out with different tools than for the Sun. These problems will also exist for seismology of Corot stars. Problems and prospects related to rapid rotation was the topic of the present paper. It is important to realize that the classification of slow, moderate or fast rotation, when oscillations are concerned, depends on the rotation rate of the star and on the frequency range of its excited oscillations, that-is on the type of stars.

For instance *intermediate mass* stars such as δ Scuti stars, have their excited frequencies and rotation rates which yield ϵ in the range 0.1-0.5. Fast rotation corresponds approximatively to $\epsilon_{max} \sim 0.2 - 0.3$ The region they fall in the $\epsilon - \mu$ diagram (Fig.24) shows that for the lowest rotating δ Scuti stars rotation can still be treated as a perturbation provided

higher order contributions ($O(\Omega^2), O(\Omega^3)$ and near-degeneracy (or truncated formulation) rather than simple perturbation approximation are included. For the fatstest rotators, on the other hand $v > 150km/s$, a non perturbative approach is necessary for quantitative comparison with observations.

For SPB and γ Dor stars, although their ritation rate is small, excited modes are low frequency g-modes. The consequence is that whereas the cengrifugal force can be neglected, μ is large (Fig.24) and the effect of the Corioilis force cannot be treated as a perturbation (Dintrans, Rieutord, 2000)

For many solar like stars, the rotation is expected to be slightly larger than for the Sun but they are still rotating much slower than A-F stars. Excited modes of solar like oscillators are high frequency p-modes which are confined to the surface where the rotation effects are larger. Strictly speaking, values of ϵ and μ are small for these stars. One must however keep in mind that distorsion effects due to the centrifugal force linearly increase with frequency and become significant for high frequency modes when the required accuracy on the computed frequencies must match that of (CoRoT) observations For these stars, higher order frequency corrections due to rotation must be taken into account when $\epsilon > \epsilon_{max} \sim 0.035 - 0.04$ (for a $1.4M_{\odot}$). μ is too small and corrections due to Coriolis are negligible. As shown in Fig.epsmu, a few stars are located at the limit $\epsilon \sim 0.035 - 0.04$. As the $\epsilon - \mu$ values have been obtained for a lower limit of the rotation rate (ie $v \sin i$), it is likely that for some of them including high order frequency corrections due to rotation will be necessary.

The hope is that seismology will help to detect localized rotation gradients and a measure of their magnitudes. This will be even more efficient if information about the surface rotation rate is available independently. A large amount of work remains to be done before seismic studies can be as fruitful as expected: deeper studies about effect of rotation on mode visibility, mode identification, mode excitation and mode selection; studies of fast rotation for realistic stellar models, quantitative studies of PMS evolution of the rotation profile and transport of angular momentum to name a few.

Acknowledgements: Most of the work described in the present paper has been financially supported by the french PNPS (Programme de Physique stellaire). We also thank the french-spanish cooperation for financing visit exchanges.

REFERENCES

1. Aerts,C.; Waelkens,C.; Daszynska-Daszkiewicz,J. et al., 2004, A&A 415, 241

2. Ausseloos, M., Scuflaire, R., Thoul., A., et al., 2004, MNRAS 355, 352

3. Baglin,A.; TheCOROTTeam, 1998, IAUS., 185, 301

4. Browning, M.K, Brun, AS, Toomre, J, 2004, ApJ, 601, 512

5. Brun, A. S.; Browning, M. K.; Toomre, J., 2005, ApJ 629, 461

6. Charbonnel, C., Talon, S., 2005, Sciences

7. Christensen-Dalsgaard,J., 1993, GONG 1992, in ' Seismic Investigation of the Sun and Stars' Editor, Timothy M. Brown; ASPC 42, 347

8. Cutispoto, G., Pastori, L., Pasquini, L., et al., 2002, A&A 384, 491

9. Daszynska-Daszkiewicz , J., Dziembowski, W.A., Pamyatnykh, A.A., Goupil, M.J., 2002, A&A 392, 151

10. DeMedeiros,J.R.; Mayor,M., 1999, A&AS 139, 433

11. Dintrans, B., Rieutord, D., 2000, A&A 354, 86

12. doNascimento,J.D.,Jr.; Charbonnel,C.; Lbre,A.; deLaverny,P.; DeMedeiros,J.R. 2000, A&A 357, 931

13. Domiciano de Souza, A., Kervella, P., Jankov, S., Vakili, F., Ohishi, N., Nordgren, T.E., Abe, L. 2005, A&A, 442, 567 !Achernar

14. Donati,J.-F.; CollierCameron,A.; Petit,P., 2003, MNRAS 345, 1187

15. Dupret,M.-A.; Thoul,A.; Scuflaire,R.; et al., 2004, A&A 415, 251

16. Dupret et al. 2005

17. Dziembowski, W.A., Goode, P., 1992, ApJ 394, 670 (DG92)

18. Dziembowski, W.A. & Goupil, M.J., 1998, The First MONS Workshop: Science with a Small Space Telescope, held in Aarhus, Denmark, June 29 - 30, 1998, Eds.: H. Kjeldsen, T.R. Bedding, Aarhus Universitet, p. 69

19. Espinosa, F., Perez-Hernandes, F., Roca-Cortès, T , 2004, Proc. of SOHO 14/GONG 2004, New Haven, USA, ESA SP 559.

20. Fremat, Y., Zorec, J., Hubert, A.M., Floquet, M., 2005, 440, 305

21. Fremat, Y., Neiner, C., Hubert, A.M., et al., 2006, A& A 451, 1053

22. Gies,D.R.; Huang,W., 2004, IAUS 215, 57G

23. Goupil, M.J., Dziembowski, W. A., Pamyatnykh, A. A., Talon, S., 2000, in Delta Scuti and Related Stars, Reference Handbook and Proceedings of the 6th Vienna Workshop in Astrophysics, held in Vienna, Austria, 4-7 August, 1999. ASP Conference Series, Vol. 210. Eds M. Breger and M. Montgomery. (San Francisco: ASP) ISBN: 1-58381-041-2, p.267

24. Goupil, M. J., Talon, S. , 2002, in Radial and Nonradial Pulsations as Probes of Stellar Physics, ASP Conference Proceedings, Vol. 259. Eds C. Aerts, T. R. Bedding, & J. Christensen-Dalsgaard. ISBN: 1-58381-099-4. Also IAU Colloquium 185. (San Francisco: ASP), p.306

25. Goupil,M.J.; Samadi,R.; Lochard,J.; Dziembowski,W.A.; Pamyatnykh,A., 2004, Second Eddington Workshop: Stellar structure and habitable planet finding. Edited by F. Favata, S. Aigrain and A. Wilson. ESA SP-538, Noordwijk: ESA Publications Division, ISBN 92-9092-848-4, 2004, p. 133

26. Goupil,M.-J.; Dupret,M.A.; Samadi,R.; Boehm,T.; Alecian,E.; Suarez,J.C.; Lebreton,Y.; Catala,C., 2005, JApA, 26, 249G

27. Karami K., Christensen-Dalsgaard, J., Pijpers, F.P., et al. , 2005, astroPh

28. Lignières, F., Rieutord, M., Reese, D., 2006, A&A in press

29. Maeder, A., Meynet, G. 2000, ARA&A, 38, 143

30. Maeder, A., Meynet, G. 2001, 373, 555

31. Maeder, A., 2003, Conf. Ser. 337, p. 15A&A 399, 263 ! Dh

32. Maeder, A., 2006, EDP Sciences, Cargese school ! Dh

33. Marsden,S.C.; Donati,J.-F.; Semel,M.; Petit,P.; Carter,B.D., 2006, MNRAS 643, 1365

34. Martayan, C., Fremat, Y., Hubert, A.M., et al. 2006 A&A 452, 273

35. Matias, J., Zahn, J.P., 1998, in Sounding solar and stellar interior s, eds J. Provost, F.X.Schmider, IAU Symp 181, poster volume

36. Mathis, S., Zahn, J.P., 2004, A&A 425, 229

37. Mathis, S., Palacios, A., Zahn, J.P., 2004, A&A 425, 243 !Dh 1.5 Msol

38. Mathis, Zahn, 2005, A&A 653, 666

39. Meynet, G., Maeder, A., 2005, in 'The Nature and Evolution of disks Around Hot Stars around hot stars', Eds R. Ignace & K. Gayley, ASP Conf. Ser. 337, p. 15

40. Meynet, G., Maeder, A. 2006, in 'Stars with the B[e] phenomenon', M. Kraus and A. Miroshnichenko (eds.), ASP Conf. Ser., in press, astro-ph/0511269

41. Meynet, G., Maeder, A., 2000, A&A 361, 101 ! massive stars

42. Morel, P., Thevenin, F., 2002 A&A 390, 611

43. Morel, P., 1997, A&AS 124 597M

44. Neiner, C., Hubert, A.M., Fremat, Y., et al., A&A 2003 409, 275

45. Owocki, S.P., 2004, in "Stelalr Rotation", IAU Symp. 215, A.Maeder, Ph. Eenens (eds), ASP

46. Palacios, A., Talon, S., Charbonnel, C., Forestini, M., 2003, A&A 399, 603

47. Pamyatnykh, A.A., Handler, G., Dziembowski, W.A., 2004, MNRAS, 350, 1022

48. Petit, P., Donati, J.F., Wade, G.A. et al., 2004, MNRAS 348, 1175

49. Petit, P., Donati, J.F., Oliveira, J.M., et al., 2004, MNRAS 351, 826

50. Penny, L.R., Sprague, A.J., Seago, G., et al 2004, ApJ 617, 1316

51. Poretti, E.; Alonso, R.; Amado, P. J.; Belmonte, J. A.; Garrido, R.; Martn-Ruiz, S.; Uytterhoeven, K.; Catala, C.; Lebreton, Y.; Michel, E.; Surez, J. C.; Aerts, C.; Creevey, O.; Goupil, M. J.; Mantegazza, L.; Mathias, P.; Rainer, M.; Weiss, W. W., 2005, AJ 129, 2461

52. Reese, D., Lignières, F., Rieutord, M., 2006, A&A in press

53. Reiners,A.; Schmitt,J.H.M.M., 2003, A&A 412, 813R

54. Royer, F., Gerbaldi, M., Faraggiana, R., Gomez, A.E. , 2002a A&A 381, 105

55. Royer, F., Grenier, S., Baylac, M.O., Gomez, A.E., Zorec, J., 2002b, A&A 393, 897

56. Roxburgh,I.W., 2004, A&A , 428, 171

57. Straka, C.W., Demarque, P., Guenther, D.B., et al, 2005 ApJ

58. Strassmeier, K.G., Pichler, T., Weber, M., et al. 2003, A&A 411, 595

59. Soufi, F., Goupil, M.J., Dziembowski, W. A., 1998, A&A 334, 911 (SGD98)

60. Suarez, J.C., Goupil, M.J., Morel, P., 2006, A&A 449, 673

61. Talon, S., Zahn, J.P., 1997, A&A, 351, 582

62. Talon, S., Kumar, P., Zahn, J.P., 2002, ApJL 574, 175 ! internal wave

63. Talon, S., 2006, EDP Sciences, Cargèse school, in press

64. Talon, Charbonnel, 1998, A&A 335, 959 !hot side of Li dip

65. Talon, Charbonnel, 2003, A&A 405, 1025 ! Li dip IGW

66. Townsend, RHD, Owocki,, SP, Howarth, ID, 2004, MRAS, 350, 189

67. Unno, W. and Osaki, Y. and Ando, H. and Saio, H. and Shibahashi, H., 1989, in 'Nonradial oscillations of stars', Tokyo: University of Tokyo Press, 1989, 2nd ed.,

68. Zahn, J.P., 1992, A&A 275, 115

69. Zorec, J., Fremat, Y., Cidale, L., 2005, A&A 441, 235

References for Procyon A:

70. Barban C., Michel E., Martic M., Schmitt J., Lebrun J.C., Baglin A., Bertaux J.L., 1999, A&A 350, 617

71. Martic M., Schmitt J., Lebrun J.-C., Barban C, Connes P., Bouchy F., Michel E., Baglin A., Appourchaux T., Bertaux J.L., 1999, A&A 351, 993

72. Martic, M.; Lebrun, J.-C.; Appourchaux, T.; Korzennik, S. G., 2004, A&A 418, 295

References for Alpha Cen A:

73. Bouchy & Carrier, 2001, A&A 374, L5

74. Bouchy & Carrier, 2002, A&A 390, 205

75. Butler R.P., Bedding T.R., Kjeldsen H., McCarthy C., O'Toole S., Tinney C.G., Marcy G.W., Wright J.T., 2004, ApJ 600, L75

76. Bedding T.R., Kjeldsen H., Butler R.P., McCarthy C., Marcy G.W., O'Toole S., Tinney C.G., Wright J.T., 2004, ApJ 614, 380

References for Alpha Cen B:

77. Carrier F. & Bourban G., 2003, A&A 406, L23

78. Kjeldsen H., Bedding T.R., Butler R.P., Christensen-Dalsgaard J., Kiss L.L., McCarthy C., Marcy G.W., Tinney C.G., Wright J.T., 2005, submitted to ApJ, astro-ph/0508609

References for ηBoo:

79. Carrier, F.; Eggenberger, P.; Bouchy, F., 2005, A&A.434, 1085

References for HD49933:

80. Mosser., B., Bouchy, F.; Catala, C.; Michel, E.; Samadi, R.; Thévenin, F.; Eggenberger, P.; Sosnowska, D.; Moutou, C.; Baglin, A., 2005, A&A 431, L13

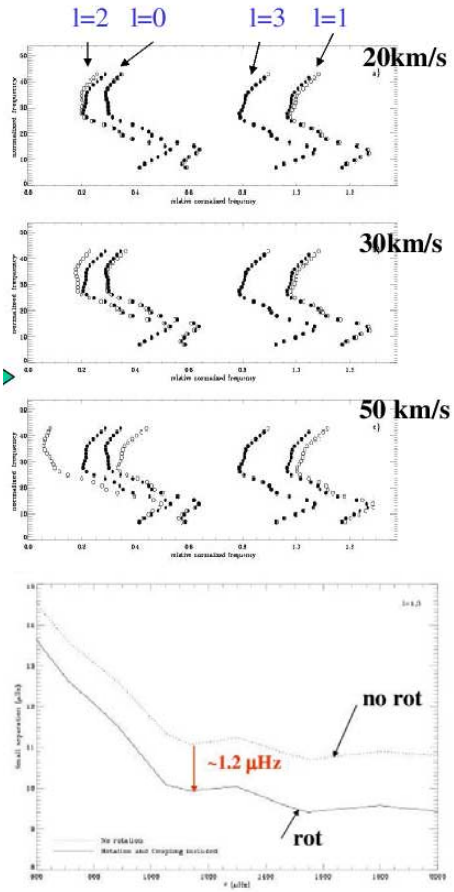

Figure 22. **top:** *Echelle diagram for a* $1.52M_{\odot}$ *model. The frequencies take into account high order effects of rotation. They are computed according to Eq. 8 and 9. The left patterns are* $\ell = 0$ *and* $\ell = 2$ *modes from left to right and the right pattern shows the* $\ell = 1, 3$ *modes from left to right.* **bottom:** *Small separations* $\nu_{n,\ell,0} - \nu_{n-1,\ell+2,0}$ *in function of the frequency* $\nu_{n,\ell,0}$ *for frequencies computed without rotation effects and including rotation effects (given by Eq.7) (from Lochard et al. 2006). Differences between both small separation reach 1.2 μHz for a rotational velocity of 30 km/s.*

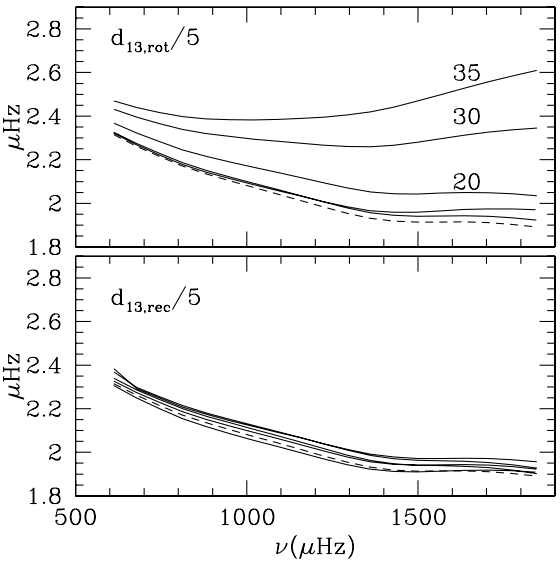

Figure 23. **top panel:** *Recovering the small separation free of pollution effects from rotation. Small separation* $nu^{(obs)}{}_{n,1,0} - \nu^{(obs)}_{n-1,3,0}$ *(Eq.7) in function of* $nu^{(obs)}{}_{n,1,0}$*. The dashed line corresponds to the small sepration calculated for frequencies without rotation. From bottom to top, the curves correspond to models with rotation velocity increasing from 0 to 35 km/s* **bottom panel**. *Small separations computed according to Eq.20. The curves now coincide with the curve obtained for the small separation computed with frequencies without rotation (from Goupil et al. 2003)*

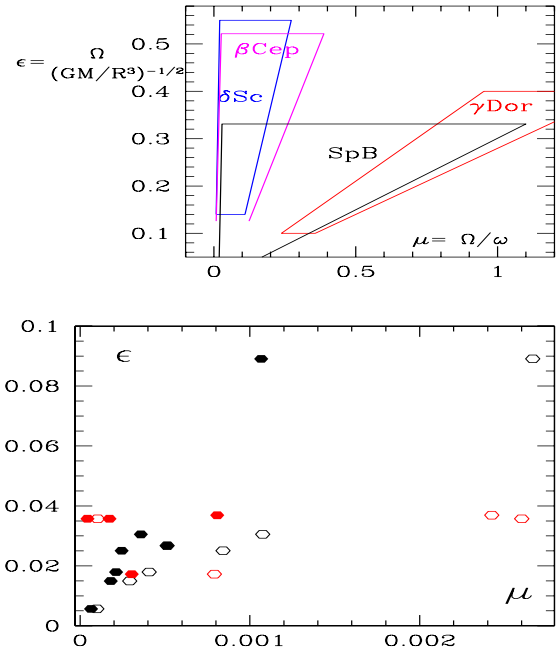

Figure 24. $\epsilon - \mu$ *diagram.* **top:** *Color delimitated areas represent regions in the* $\epsilon - \mu$ *diagram (Eq.3) cooresponding to various types of oscillating stars (from Goupil, Talon 2002). For these stars,* $\epsilon > 0.1$ *requires second and third order frequency corrections,* $\epsilon > 0.3$ *non perturbative calculation techniques.* **bottom:** *Same as the top pannel but for solar like oscillators. Dots represents* ϵ, μ *values for a set of stars which show solar like oscillations (taken from Goupil, Barban, 2006):* ϵ *Oph,* ξ *Hya,* α *Hya,* α *Hya,* α *Cen A,* α *Cen B, Procyon,* η *Boo,* μ *Arae,* β *Vir,* ζ *Her. A few among these stars are red giants. Values for* ϵ, μ *are computed using observed* $v \sin i$ *and the range of detected frequencies from the litterature: open (full) dots represent maximum (minimum) values of* μ.